About OMICS Group

OMICS Group International is an amalgamation of Open Access publications and worldwide international science conferences and events. Established in the year 2007 with the sole aim of making the information on Sciences and technology 'Open Access', OMICS Group publishes 400 online open access scholarly journals in all aspects of Science, Engineering, Management and Technology journals. OMICS Group has been instrumental in taking the knowledge on Science & technology to the doorsteps of ordinary men and women. Research Scholars, Students, Libraries, Educational Institutions, Research centers and the industry are main stakeholders that benefitted greatly from this knowledge dissemination. OMICS Group also organizes 300 International conferences annually across the globe, where knowledge transfer takes place through debates, round table discussions, poster presentations, workshops, symposia and exhibitions.

About OMICS Group Conferences

OMICS Group International is a pioneer and leading science event organizer, which publishes around 400 open access journals and conducts over 300 Medical, Clinical, Engineering, Life Sciences, Pharma scientific conferences all over the globe annually with the support of more than 1000 scientific associations and 30,000 editorial board members and 3.5 million followers to its credit.

OMICS Group has organized 500 conferences, workshops and national symposiums across the major cities including San Francisco, Las Vegas, San Antonio, Omaha, Orlando, Raleigh, Santa Clara, Chicago, Philadelphia, Baltimore, United Kingdom, Valencia, Dubai, Beijing, Hyderabad, Bengaluru and Mumbai.

Mech-Aero San Francisco (October 5th 2015)

“ Design and Assessment of Vertical Axis Wind Turbine Farms ”

Shaaban Abdallah

abdallsa@mail.uc.edu

Department of Aerospace Engineering and Engineering Mechanics
University of Cincinnati, Cincinnati, Oh 45221

University of Cincinnati

Outlines

- Introduction
- Motivation and Problem Definition
- Contribution to Knowledge
- Strategy for Problem Solution
- Results
- Conclusion
- References

Introduction

Nonrenewable and Renewable Energy Resources:

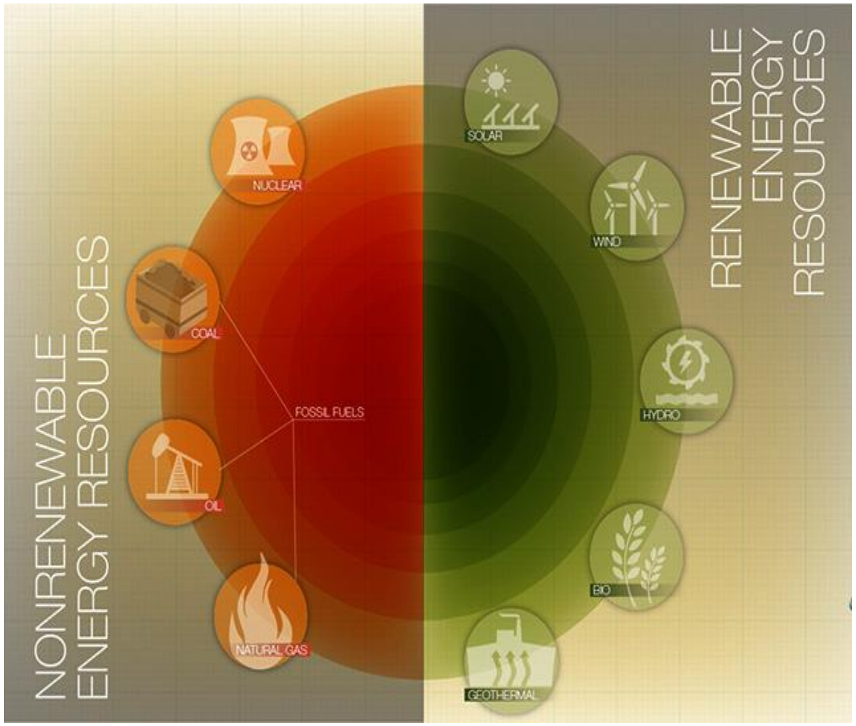

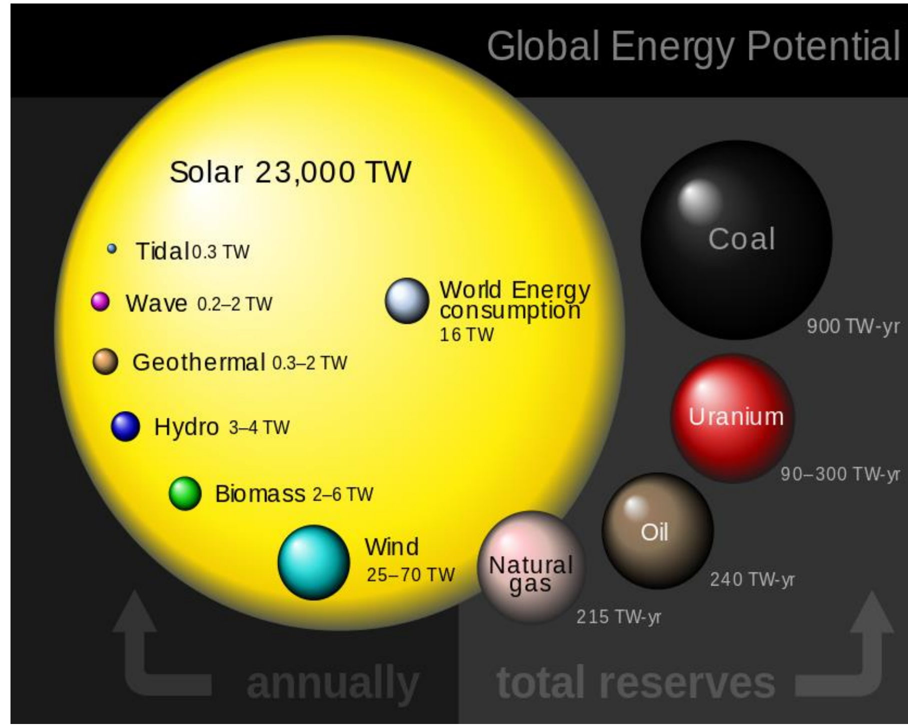

- Based on REN21's 2014 report, **renewable energy** contributed by 19% to **global energy consumption** and **22 % to electricity generation**

- The **annual** available **wind** energy is **25-70 TW**

Global Wind Energy Capacity

- "Of all the forces of nature, I should think the wind contains the largest amount of motive power "

  " Abraham Lincoln (1860)"

- The Wind energy has the fastest growing renewable power capacity

  " Renewables Global Report (2006-2012)"

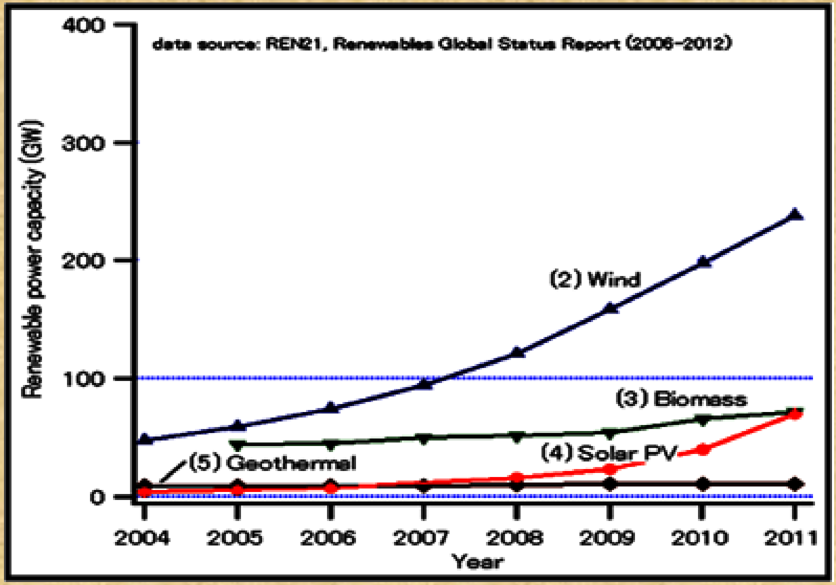

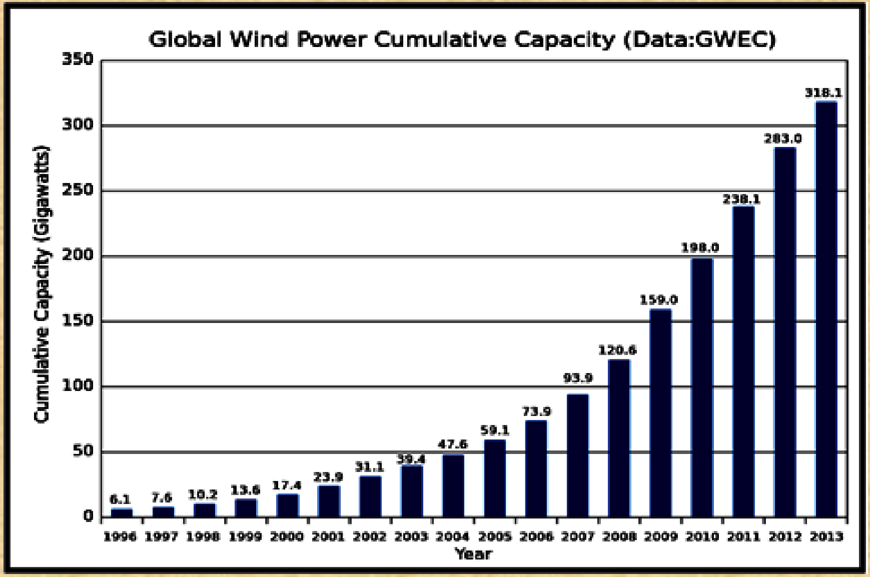

- The total worldwide wind capacity installed was 360 GW at the end of 2014, this provided 4% of the global electricity demand

  " World Wind Energy Association 2014 half year report (August 2014)"

Types of Wind Turbines:

Horizontal Axis Wind Turbines

Single Blade:

- Tower shadow effects
- Counter weights
- Less stability

Two Blades:

- less stability
- Low strength to wind shocks

Three Blades:

- Higher strength to wind storms.
- Less effect of tower shadow.
- Produces high output

Vertical Axis Wind Turbines

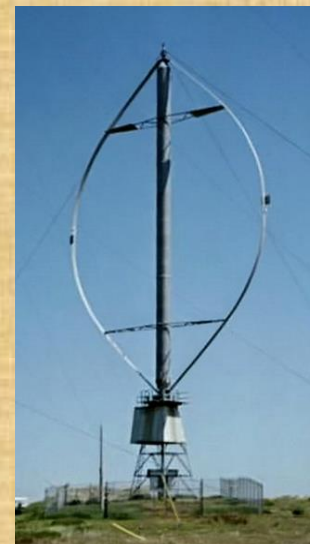

Darrieus | **H-Rotor** | **Savonius**

Horizontal Axis Wind Turbines (HAWTs) Farms:

- An isolated HAWT has the highest **power coefficient Cp (0.4–0.45)** Compared to all wind turbines

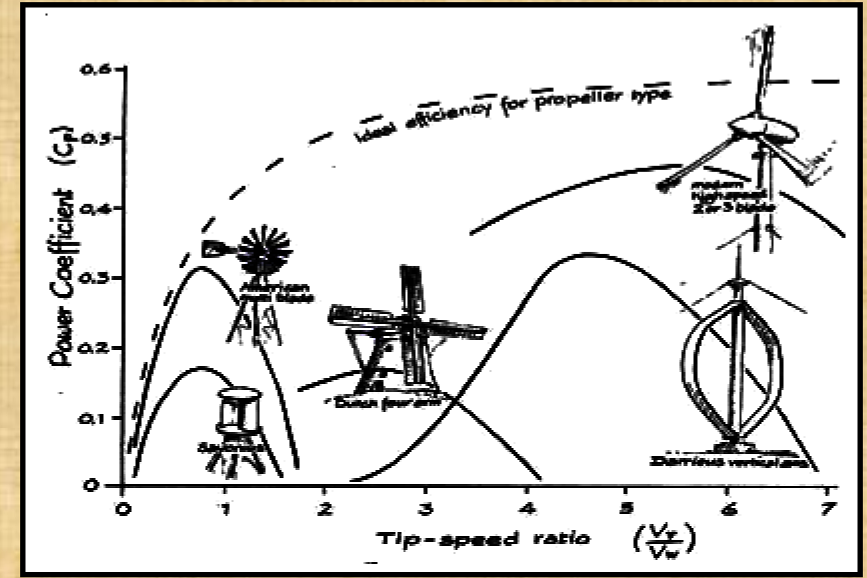

- **74%** of the wind **manufacturers** invest in **HAWTs** while only **18%** adopt the Vertical Axis Wind Turbines (**VAWTs**).

- Almost, all the **existing** wind turbine **farms** consists of **HAWTs**

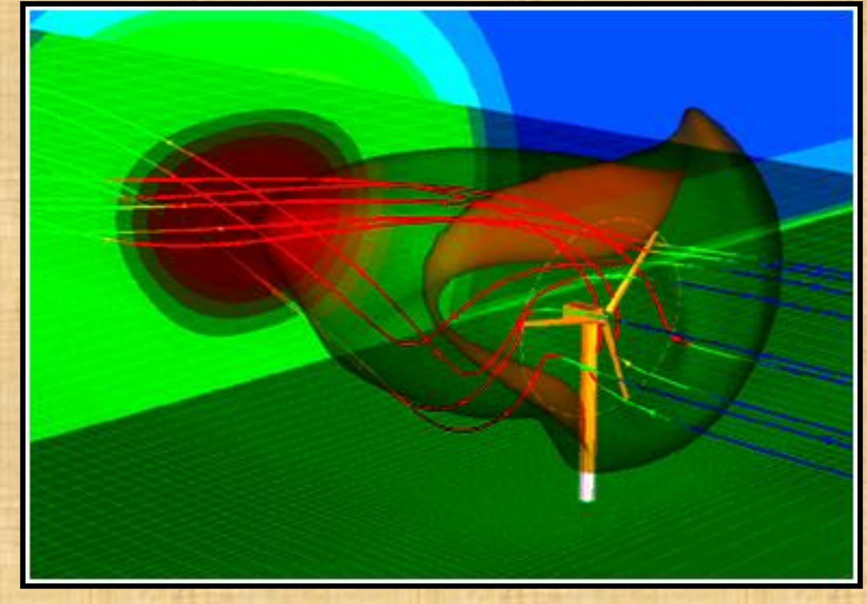

- In **close proximity** to neighboring turbines, HAWTs suffer from a **reduced power coefficient** cause by the effect of the wake of upstream turbines

Wake interactions limit Conventional Horizontal Axis Wind Turbine Farm performance

Wind Farm Power Density:

- The **power density** **(P.D.)** of a wind farm is defined as the **total power** it can generate **per unit land** area it **occupies**

$$\mathbf{P.D = \frac{Power\ Output\ of\ Farm}{Area\ of\ Farm}}$$

Vertical Axis Wind Turbine Farms

Vertical axis wind turbines (VAWTs) are proposed as an **alternative** to the more commonly used horizontal axis wind turbines (HAWTs) due to the potential increase in **power density** that is possible with VAWTs.

Experimental researches at **CalTech** found that the power density of **H-rotor** VAWT farms can be increased up to **30 W/m^2** by **optimizing the placement** of the turbines that enables them to **extract energy** from adjacent turbines **wakes**

John O. Dabiri, " Potential order-of-magnitude enhancement of wind farm power density via counter-rotating vertical-axis wind turbine arrays," Journal Of Renewable And Sustainable Energy 3: 043104 (2011)

A Numerical study on two dimensional Savonius turbine clusters, showed that a mutual enhancement between closely arranged turbines occurs as a function of :

- **Relative direction of rotation.**
- **Gap Distance between rotors (S).**
- **Relative phase angle between the rotors:**

$$\varphi = \theta 1 - \theta 2$$

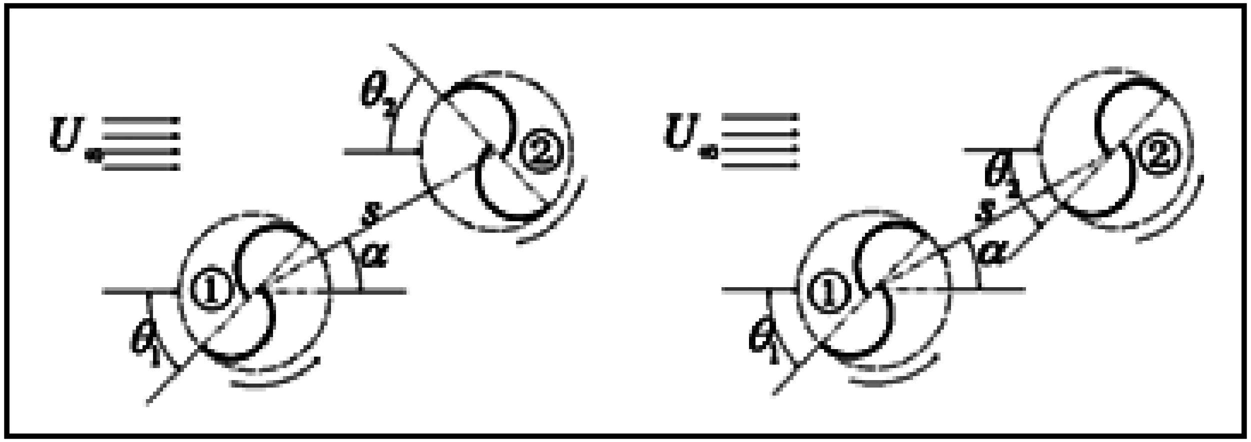

Xiaojing Sun, Daihai Luo, Diangui Huang and Guoqing Wu,"Numerical study on coupling effects among multiple Savonius turbines," Journal of Renewable and Sustainable Energy 4: 053107 (2012)

Motivation and Problem Definition

Motivation:

Previous studies showed that **VAWTs in close separation** distances mutually **enhance** their **power coefficients** resulting in **higher power output** for **individual** turbines and **higher power density** if arranged in a **wind farm**

Problem (1):

All the **previous** studies **did not extended the results** for efficient layouts of VAWTs to develop **larger efficient farms** that generate the highest possible power output keeping a high power density

Problem (2):

Using **non isolated turbines** in a farm will make the **prediction of a farm performance** to become a complicated job as each turbine will have a **different performance**

Contribution to Knowledge

Solution (1):

This study introduces the idea of the efficient VAWT **cluster as a building unit** for an **efficient VAWT** farm that generates the **highest** possible **power** using the mutual enhancement between individual turbines and has a **high power density** compared to isolated counter-part

Solution (2):

Using the efficient cluster as a building unit for the **development of efficient and patterned VAWT farms** which have the **same geometric topology** of the **cluster** provides the capability of **predicting the performance** of a farm having a geometric progression of the efficient cluster.

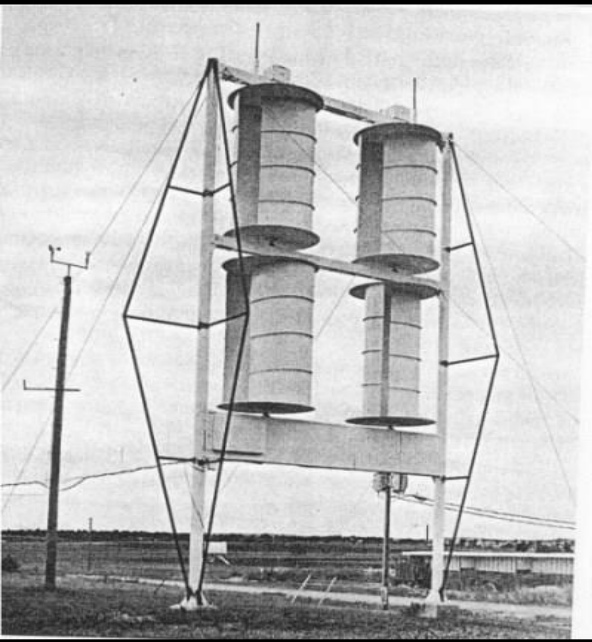

Case Study (I)

Savonius Wind Turbine

Savonius Wind Turbine

- The **Savonius** wind turbine was **invented 1929**
- It is has a **Simple Construction**
- It is a **drag-type** device
- Consists of **two** or **three buckets**
- It has **self starting capability**
- **Low noise levels** due to operation at low tips speed ratio
- Savonius turbines have **low efficiencies 15-20%**

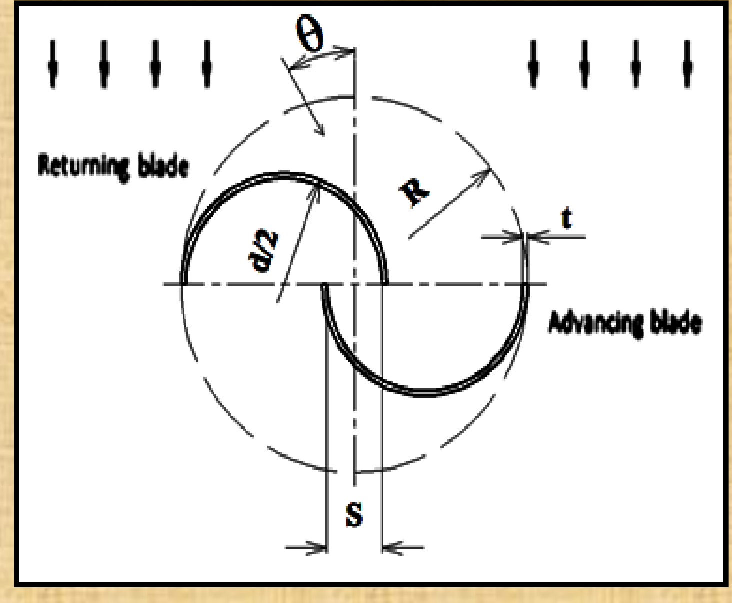

A. Shigetomi, Y. Murai, Y. Tasaka, Y. Takeda, "Interactive flow field around two Savonius turbines," Renewable Energy 36: 536-545, (2011)

Computational Domain:

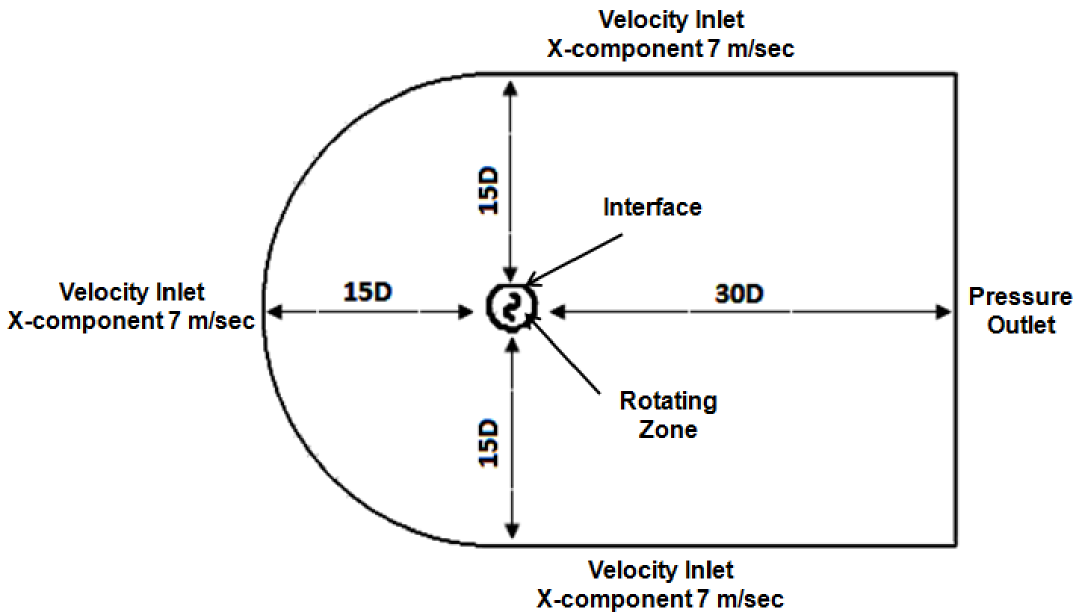

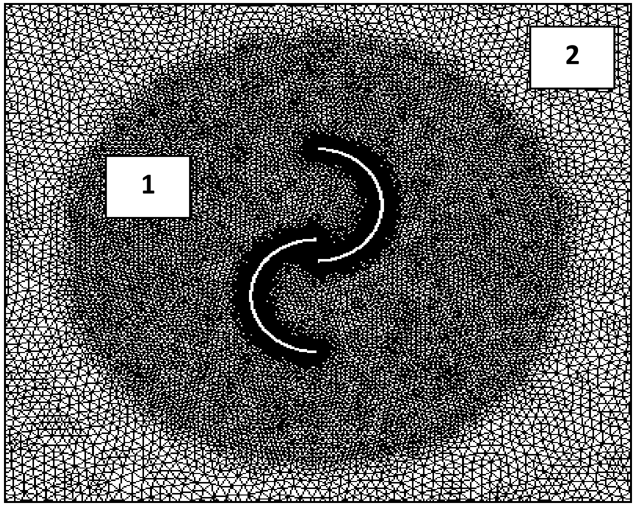

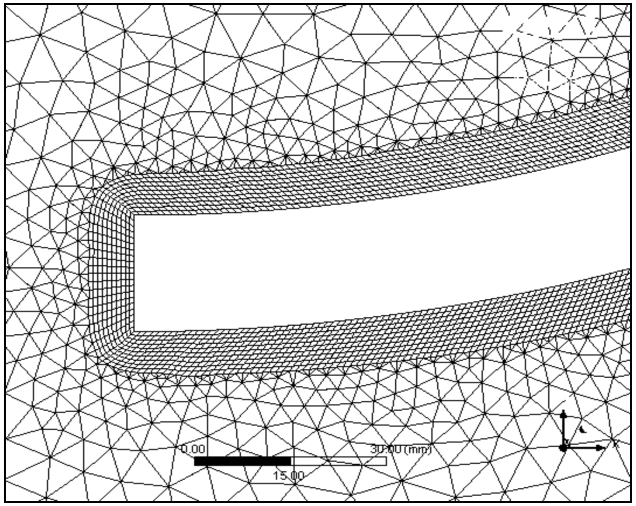

Grid Generation:

The grid structure consists of a non conformal mesh with **unstructured triangular elements** generated using ANSYS meshing.

An inflation of 10 levels of quad. cells is imposed to account for the boundary layer with a maximum thickness of 1 mm to achieve a y+ < 1 as required by the transition SST turbulence model [36, 37].

Numerical Model Validation:

Three models has been checked:

- K-ε model
- K-ω SST model
- Transition SST model

The **transition SST turbulence** model shows closer agreement to the **experiments data** in the numerical results for:

- Static torque coefficient at different azimuth angles (θ)
- Power coefficient at different tip speed ratios (λ)

The maximum power coefficient:

$\mathbf{Cp_{max}} = 0.23$ at $\lambda = 1$

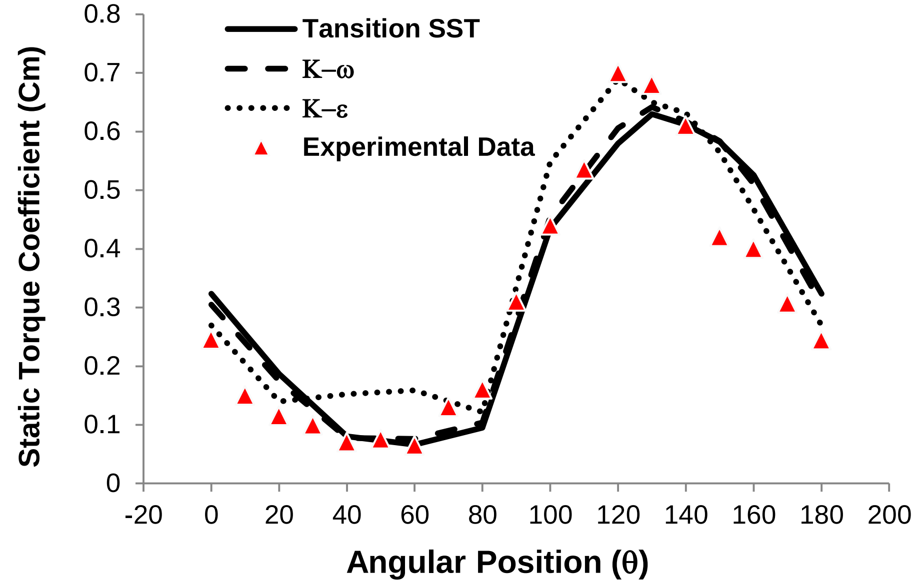

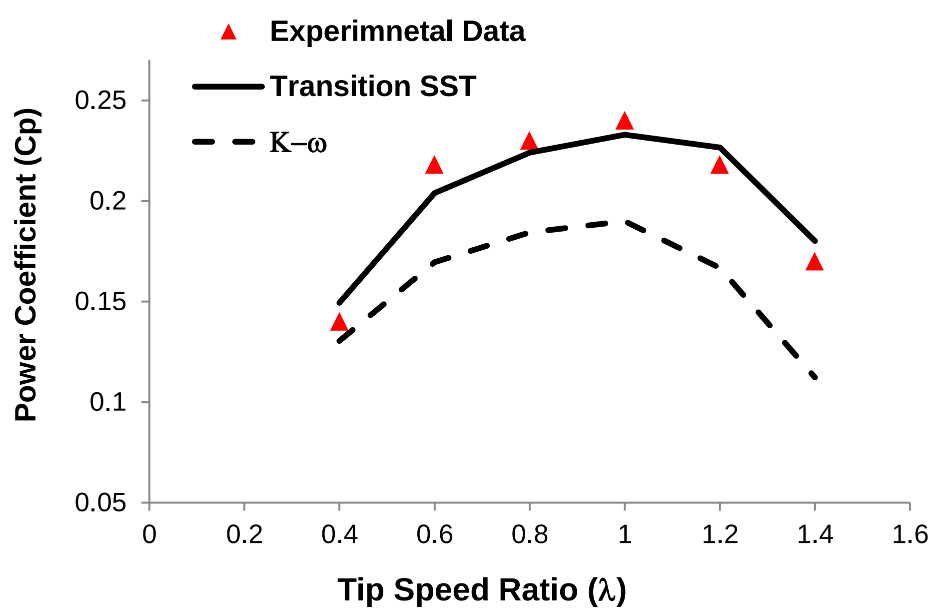

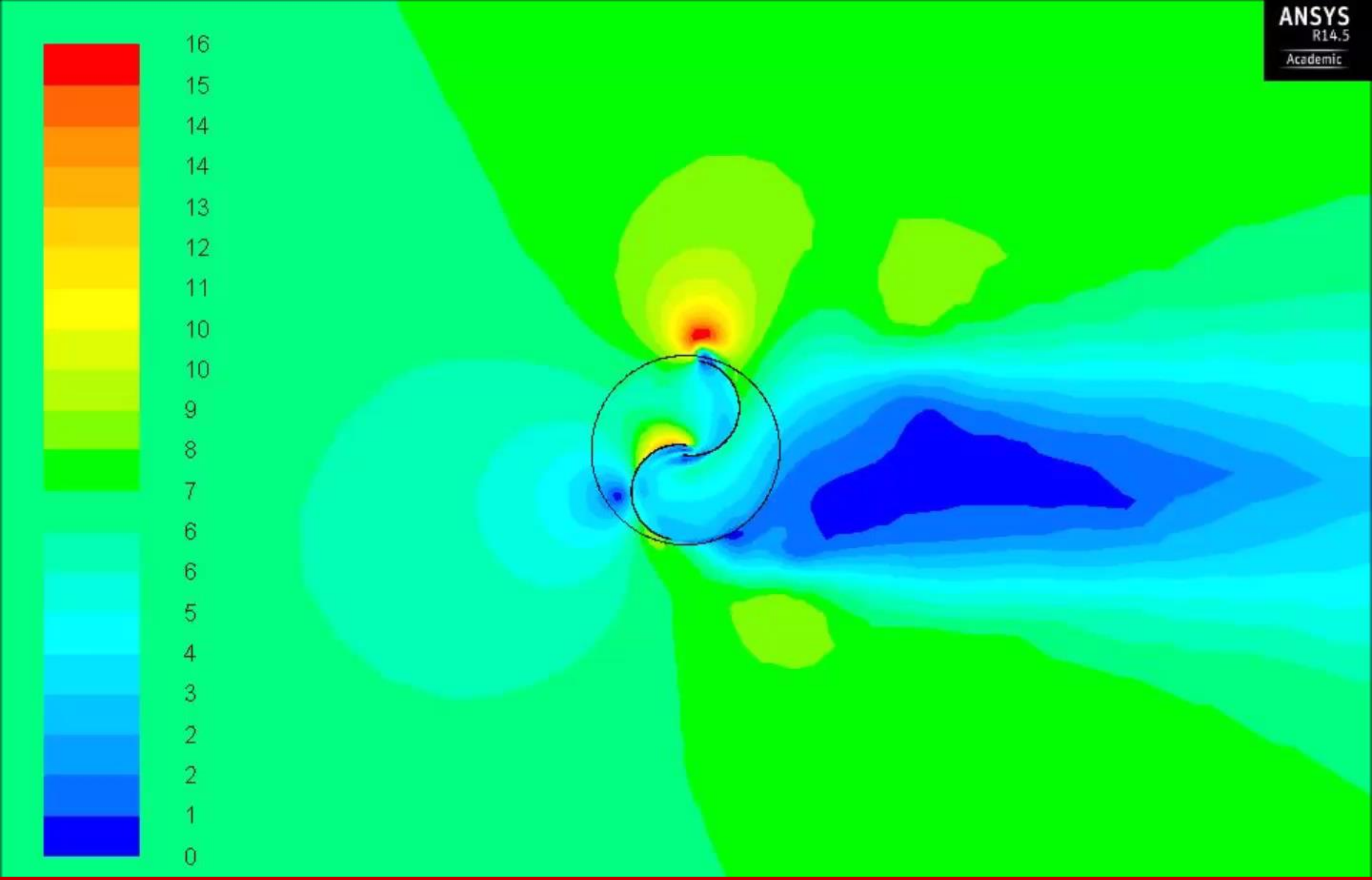

Velocity Contours: Single Savonius Turbine

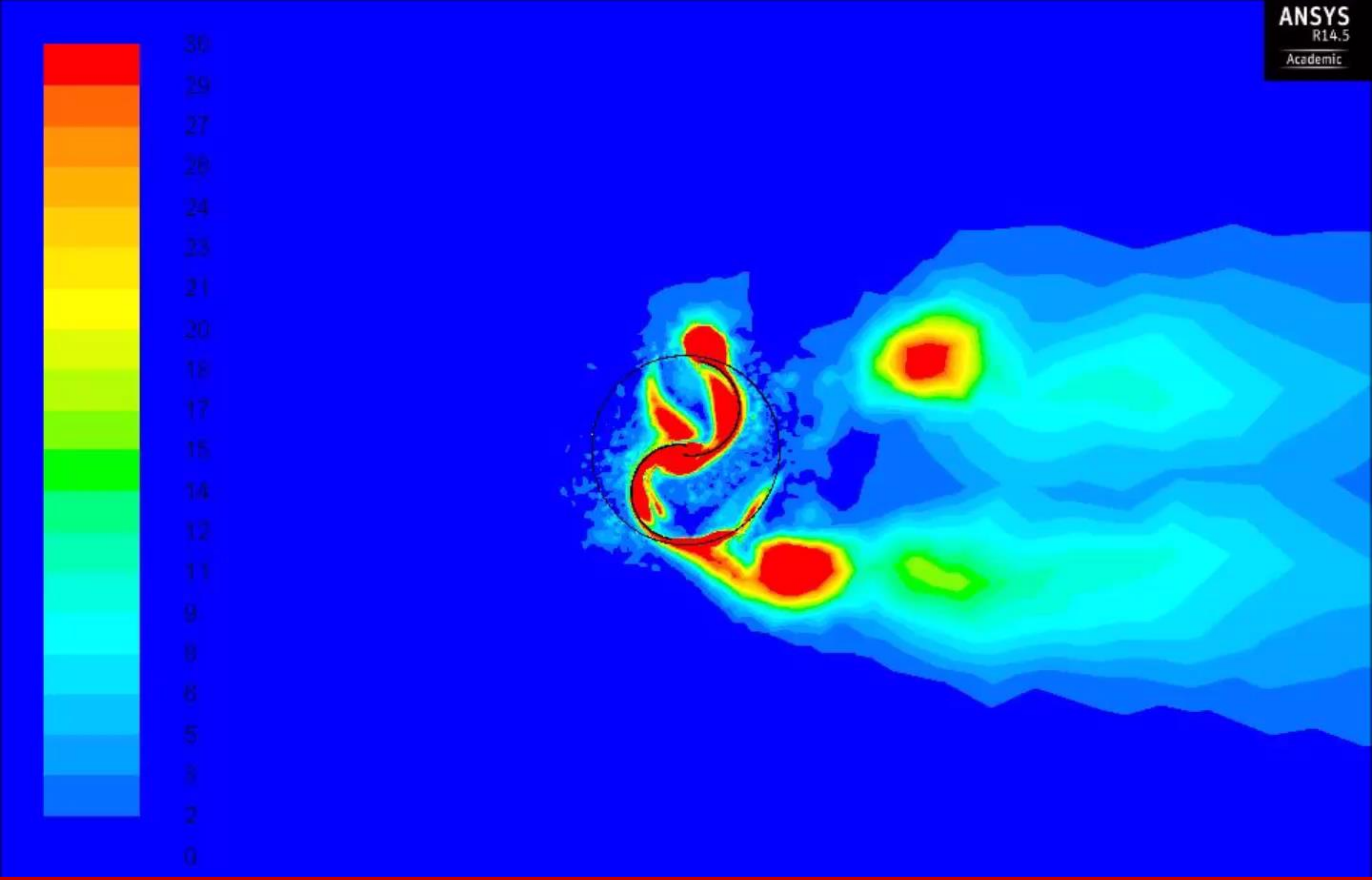

Vorticity Contours: Single Savonius Turbine

Flow Pattern around a Single Savonius Rotor

The flow patterns around the rotor are identified and found comparable to the experimental data:

- **Flow (I):** Coanda flow (Attached to the advancing blade convex side).
- **Flow (II):** Dragging flow (from the advancing blade convex side to the returning blade concave side).
- **Flow (III):** Overlap flow though the overlapping area.
- **Flow (IV):** Stagnation flow from upstream to the returning blade convex side.
- **Flow (V):** Shedding vortex at the advancing blade tip.
- **Flow (VI):** Shedding vortex from the returning blade tip.

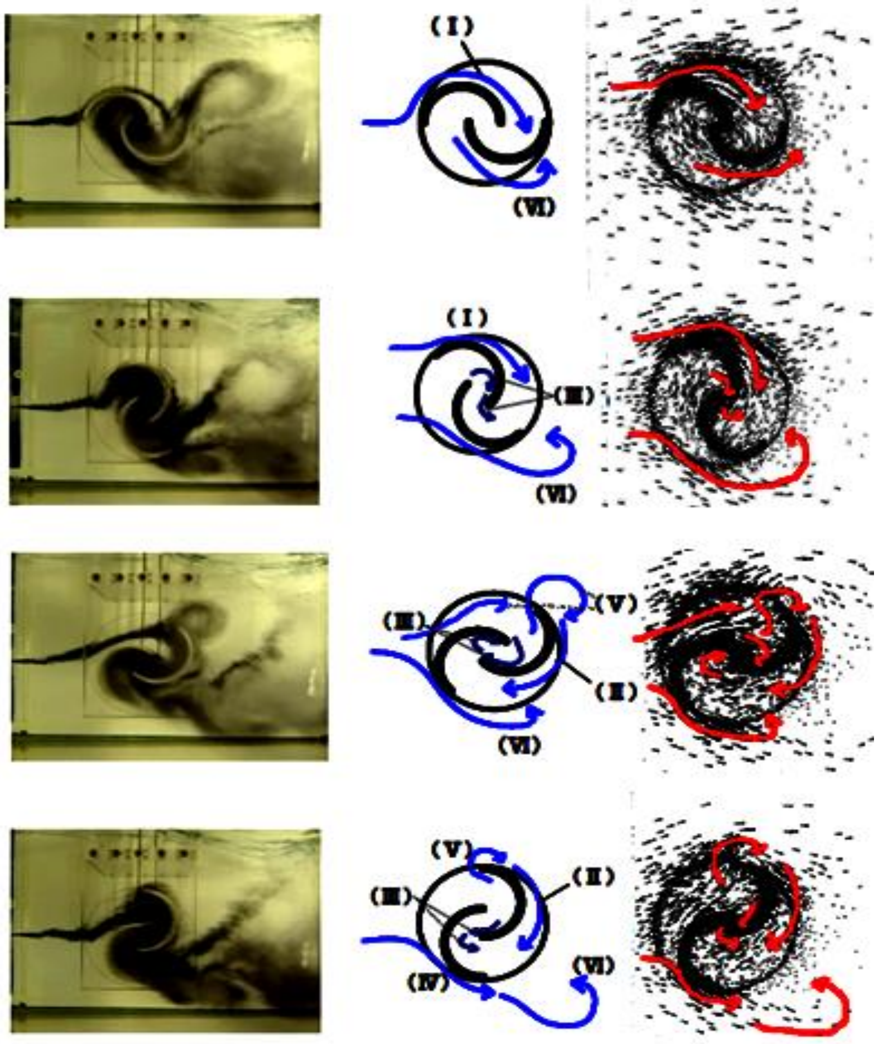

Nakajima, M., IIO, S., Ikeda, T., Performance of double-step Savonius rotor for environmentally friendly hydraulic turbine. Journal of Fluid Science and Technology 3, (2008)

3D Validation for a Single Savonius Turbine

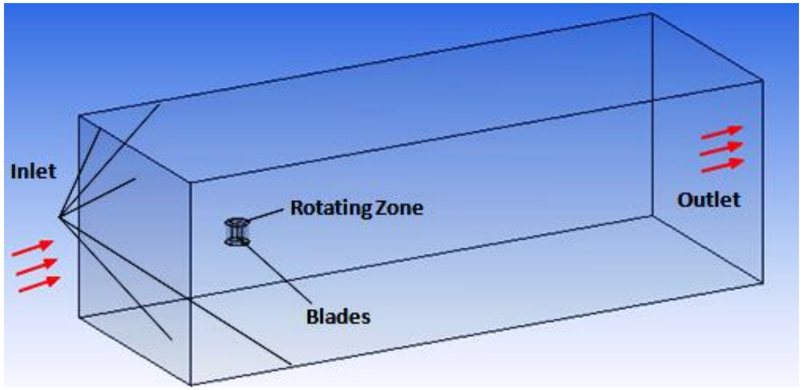

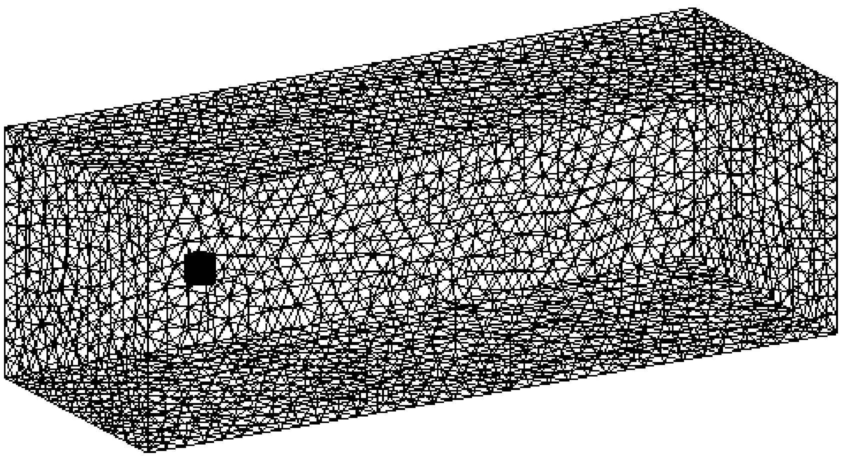

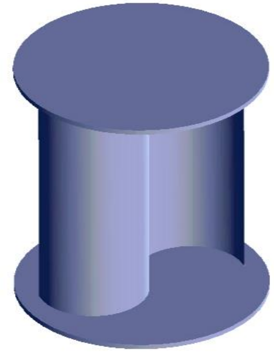

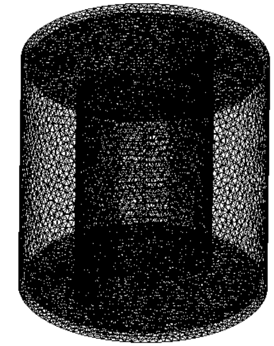

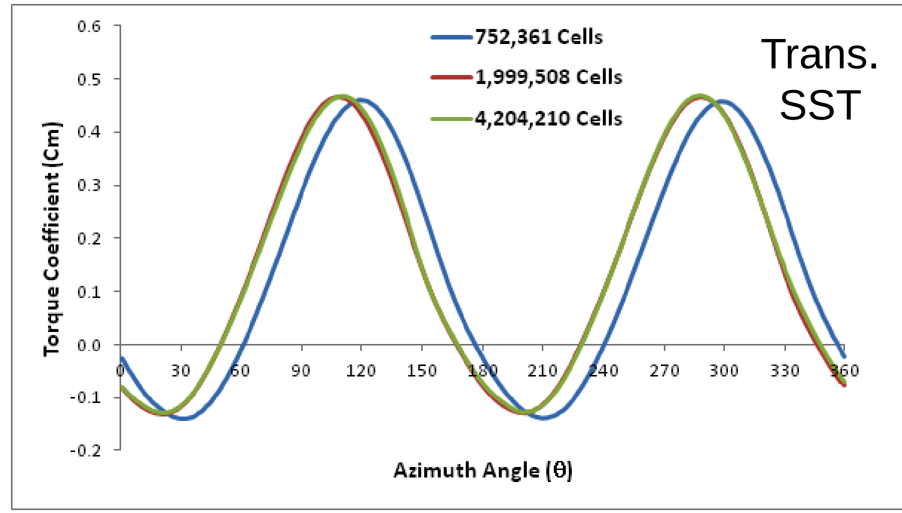

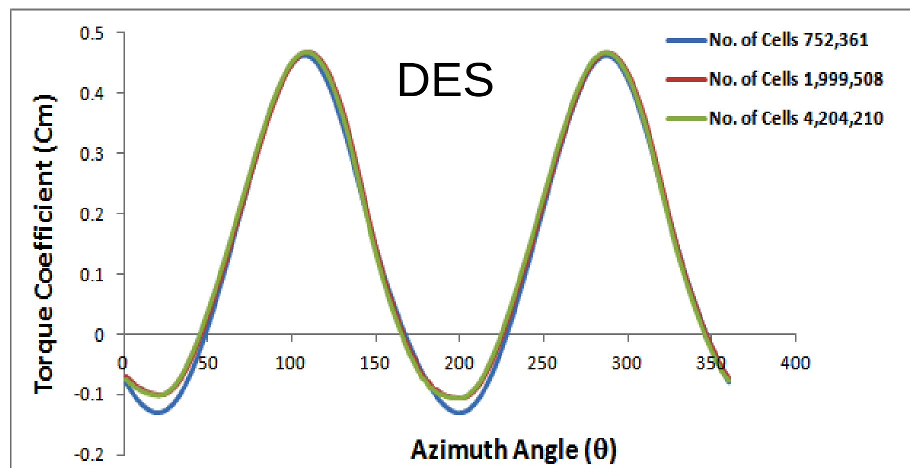

Grid Level	No. of Cells	Cm Transition SST	Cm DES
1	752,361	0.1461	0.1806
2	1,999,508	0.1561	0.1909
3	4,204,210	0.1557	0.1901

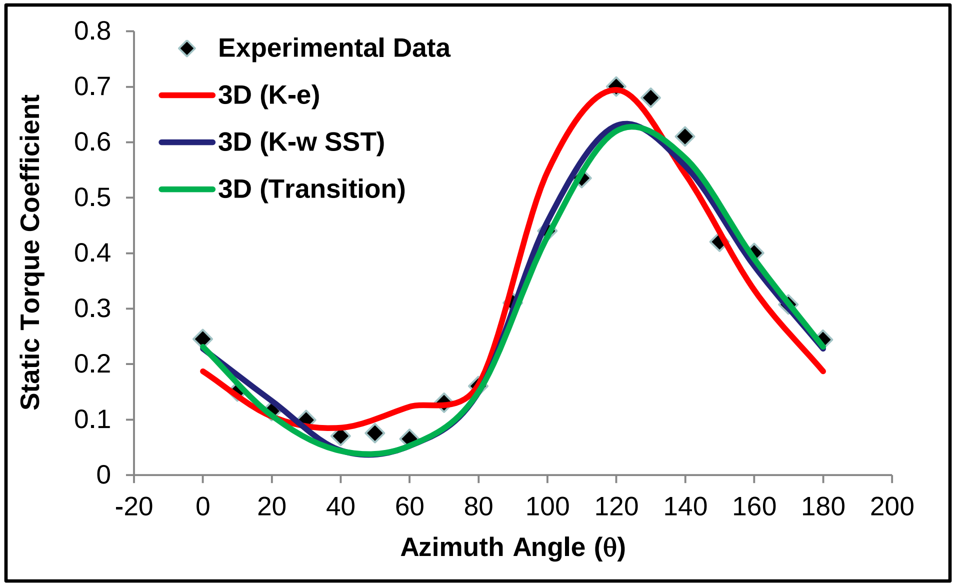

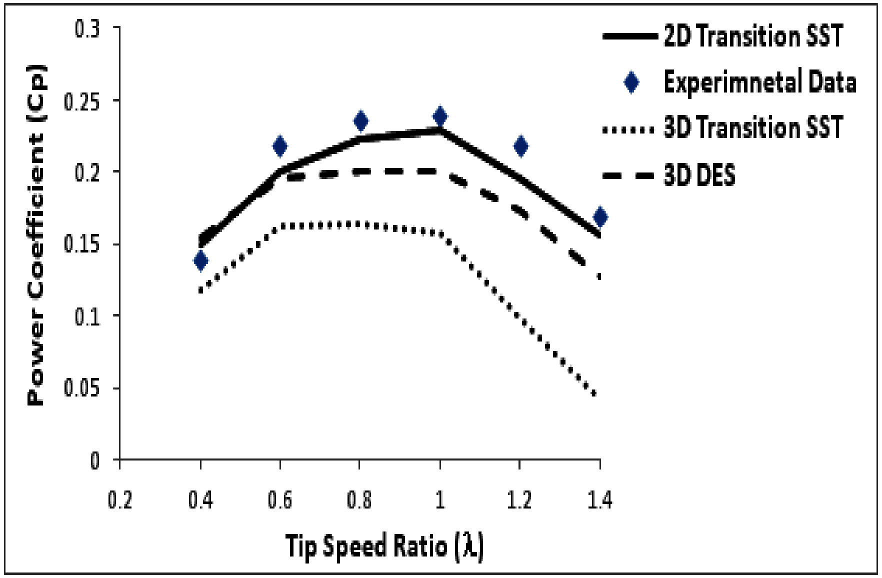

Transition SST model in the 3D Solution under predicted the single turbine performance compared to experimental data, this results are in consistence with the literature review on 3D solutions

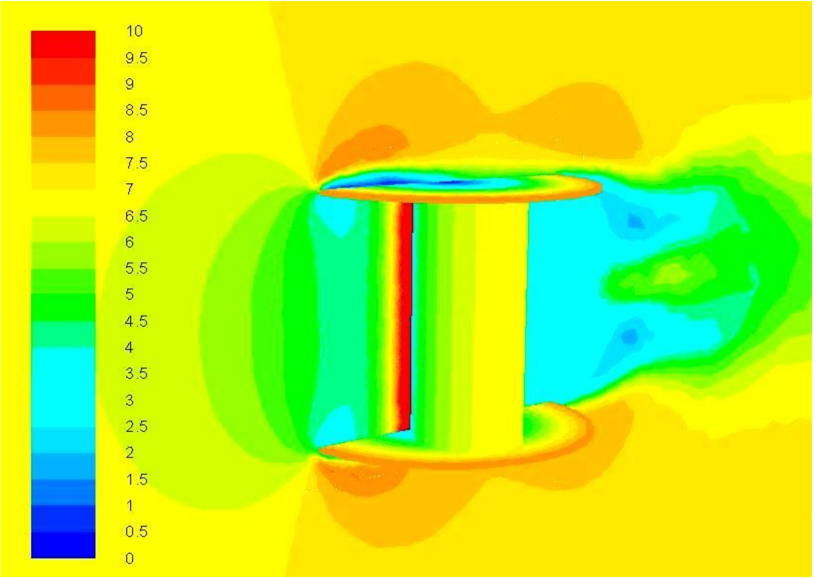

To obtain better rsults, **detached eddy simulation (DES)** model is used for the flow simulation, the obtained results are **closer to the experimental data** for different TSR

The max. difference between DES and experimental data is about 15%

Numerical Solution of Two Savonius Wind Turbine Clusters

The development of an efficient cluster requires the study of different possibilities of multiple turbine cluster

Two **Co-rotating** and **Counter-rotating** turbine clusters in parallel and oblique configurations are numerically simulated

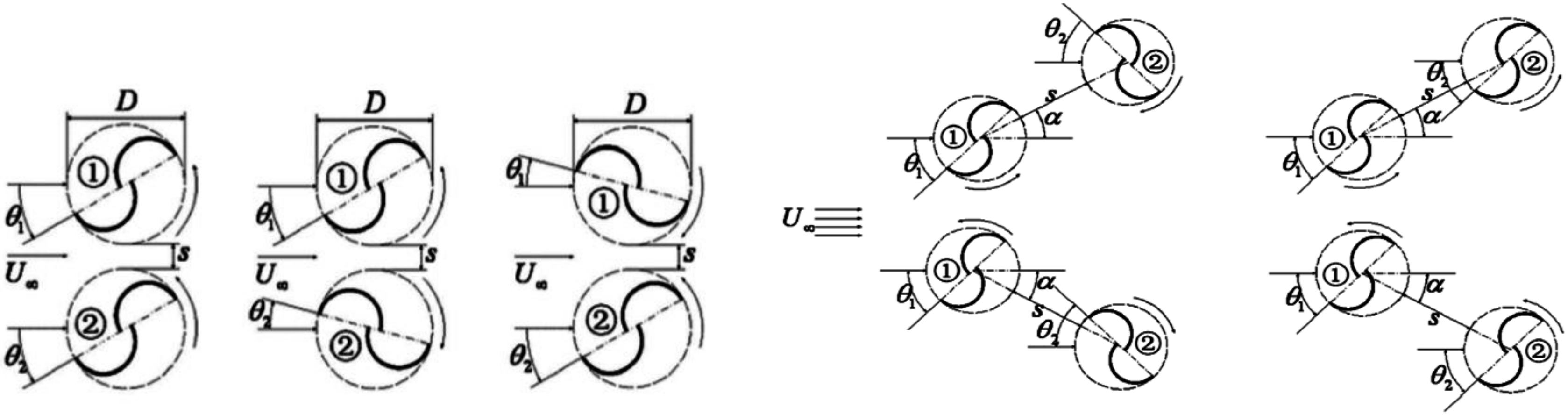

Parallel Configurations **Oblique Configurations**

Xiaojing, S., Daihai, L., Diangui, H., Guoqing, W. Numerical study on coupling effects among multiple Savonius turbines. Journal of Renewable and Sustainable Energy 4: 053107, 2012

1- Two Parallel Co-Rotating Savonius Turbines:

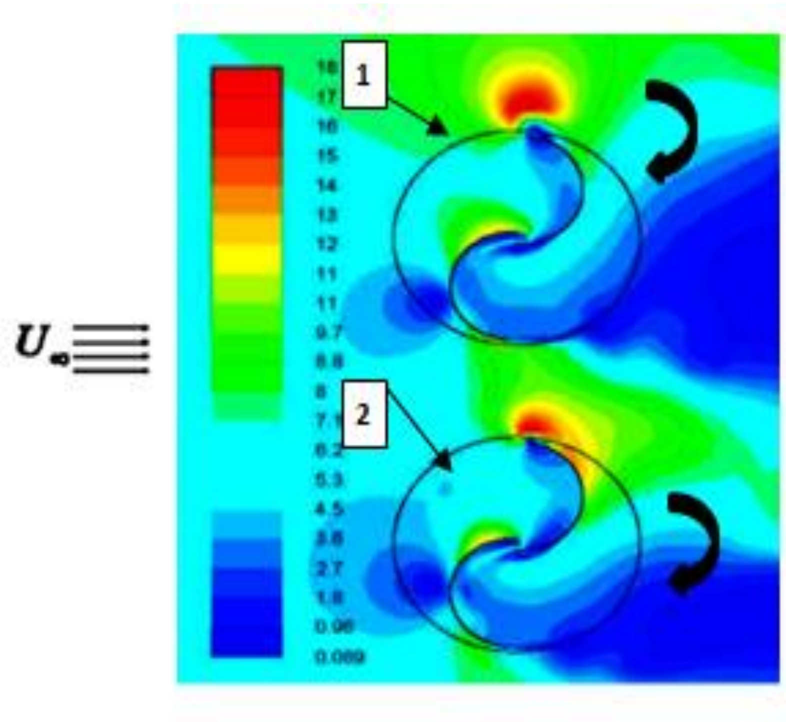

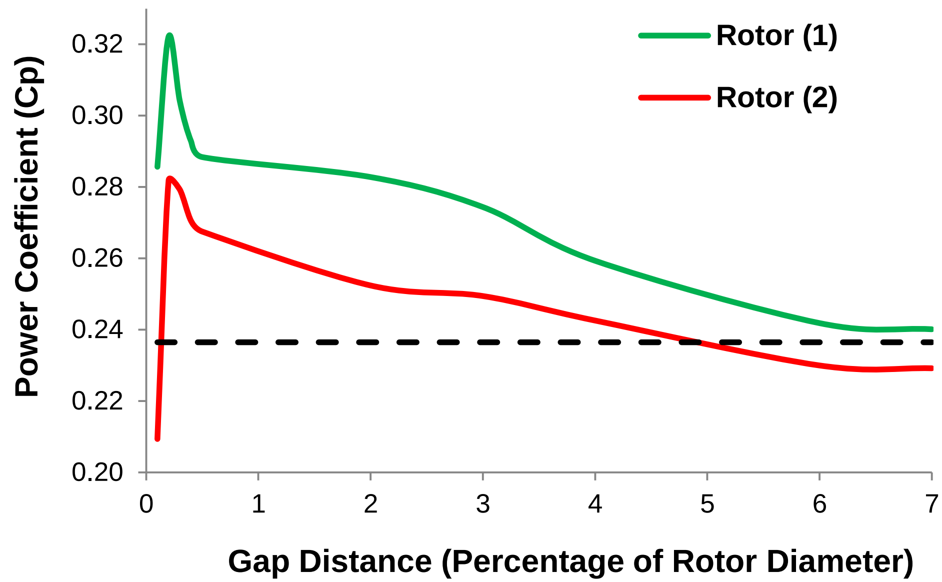

Rotor (1) has higher efficiency enhancement than Rotor (2) due to the direction of rotation

Cp_{avg} max is 0.3 at **0.2D** gap distance enhancement of **30%** higher than isolated turbines

Reaches isolated turbine performance placed at approximately 5-6 D

2- Two Parallel Counter-Rotating Savonius Turbines

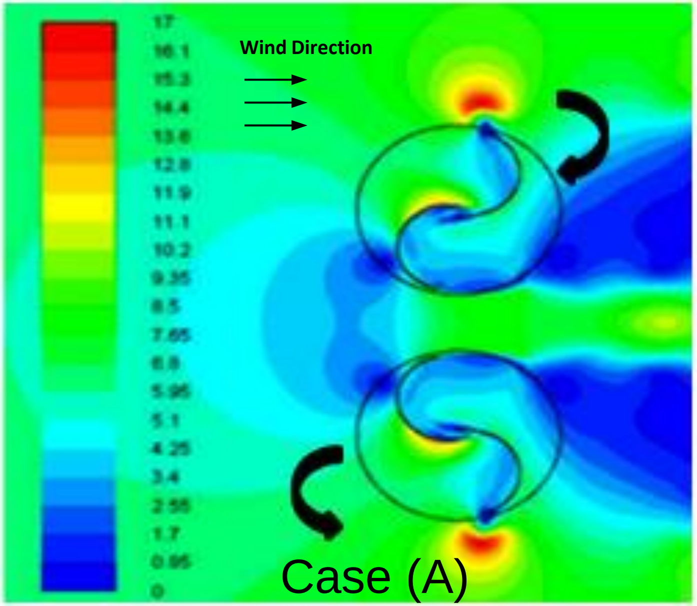

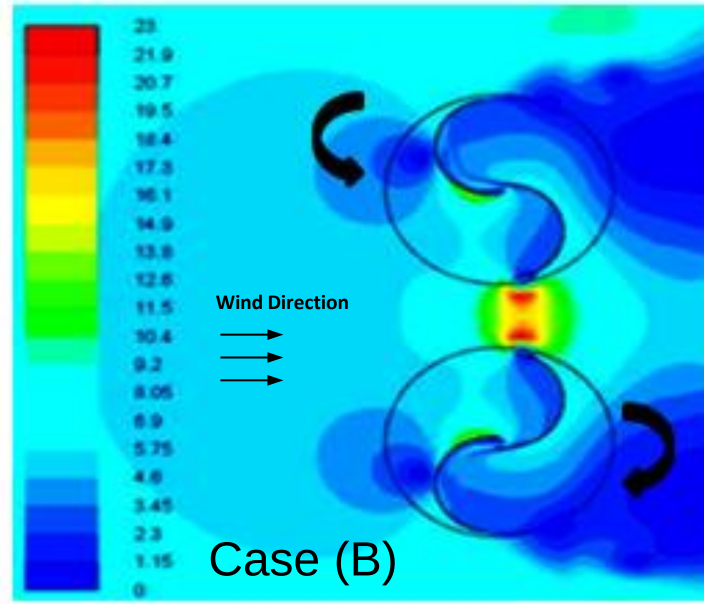

Cp_{avg} max is 0.26 at 0.8D gap distance

Cp_{avg} max is 0.3 at 0.8D gap distance

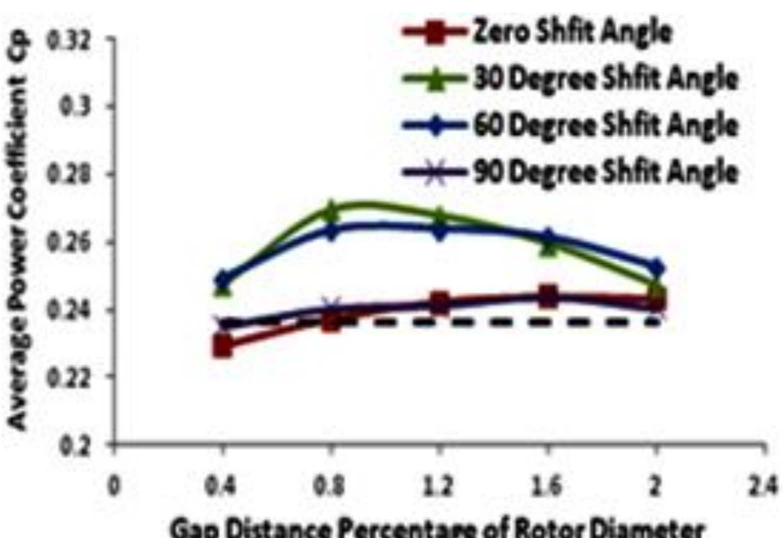

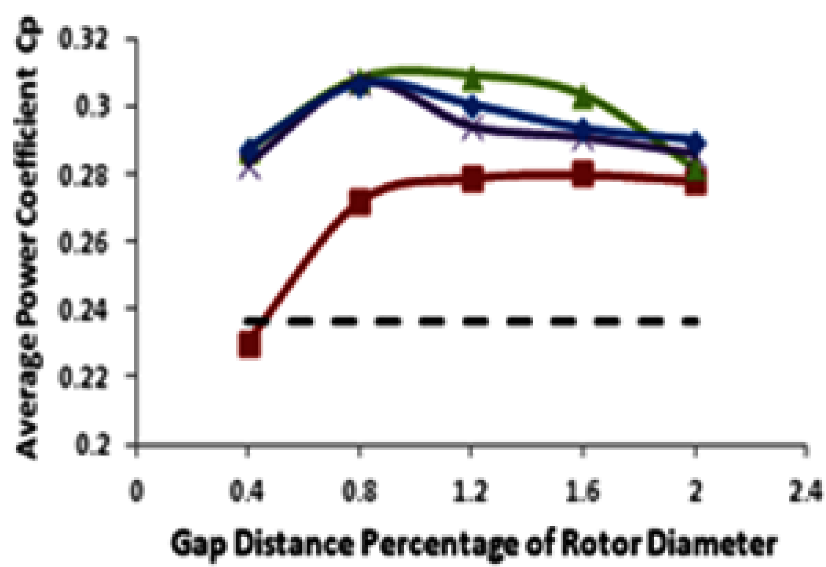

Comparison Between Co- and Counter-Rotating Two Parallel Turbines

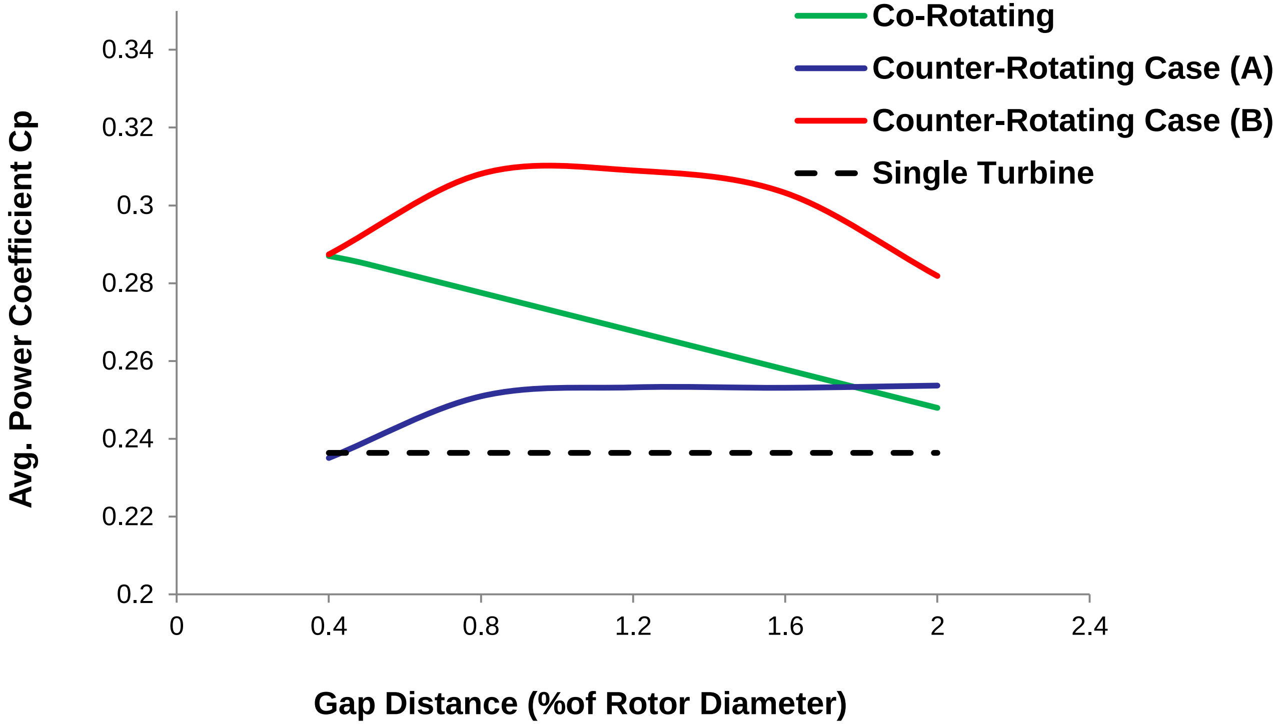

case (B) for counter-rotating rotors at a relative phase angle 30° is the most efficient for two parallel counter-rotating Savonius rotors, where the inward buckets are advancing buckets

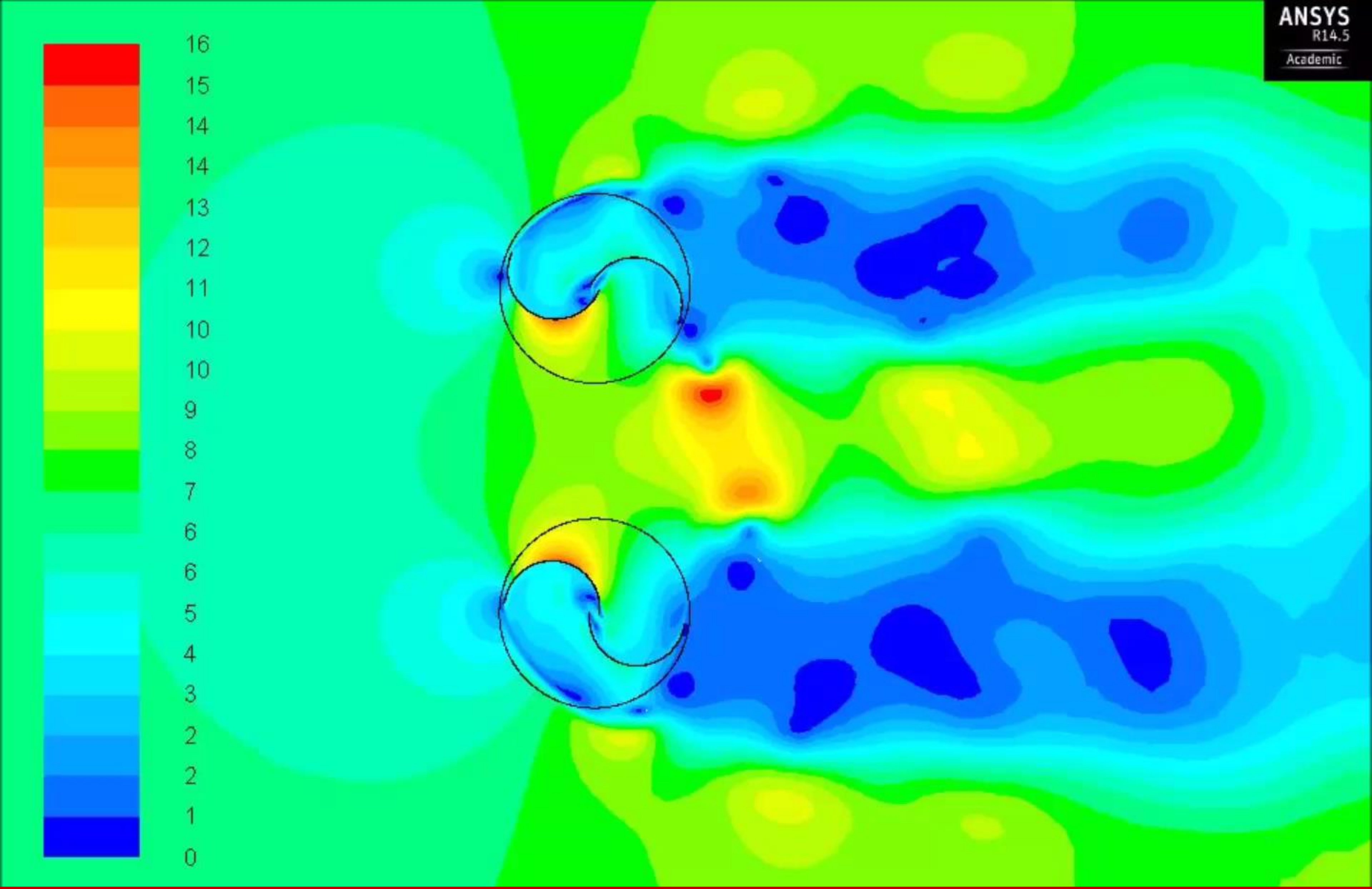

Velocity Contours: Two Parallel Counter-Rotating Savonius Turbines

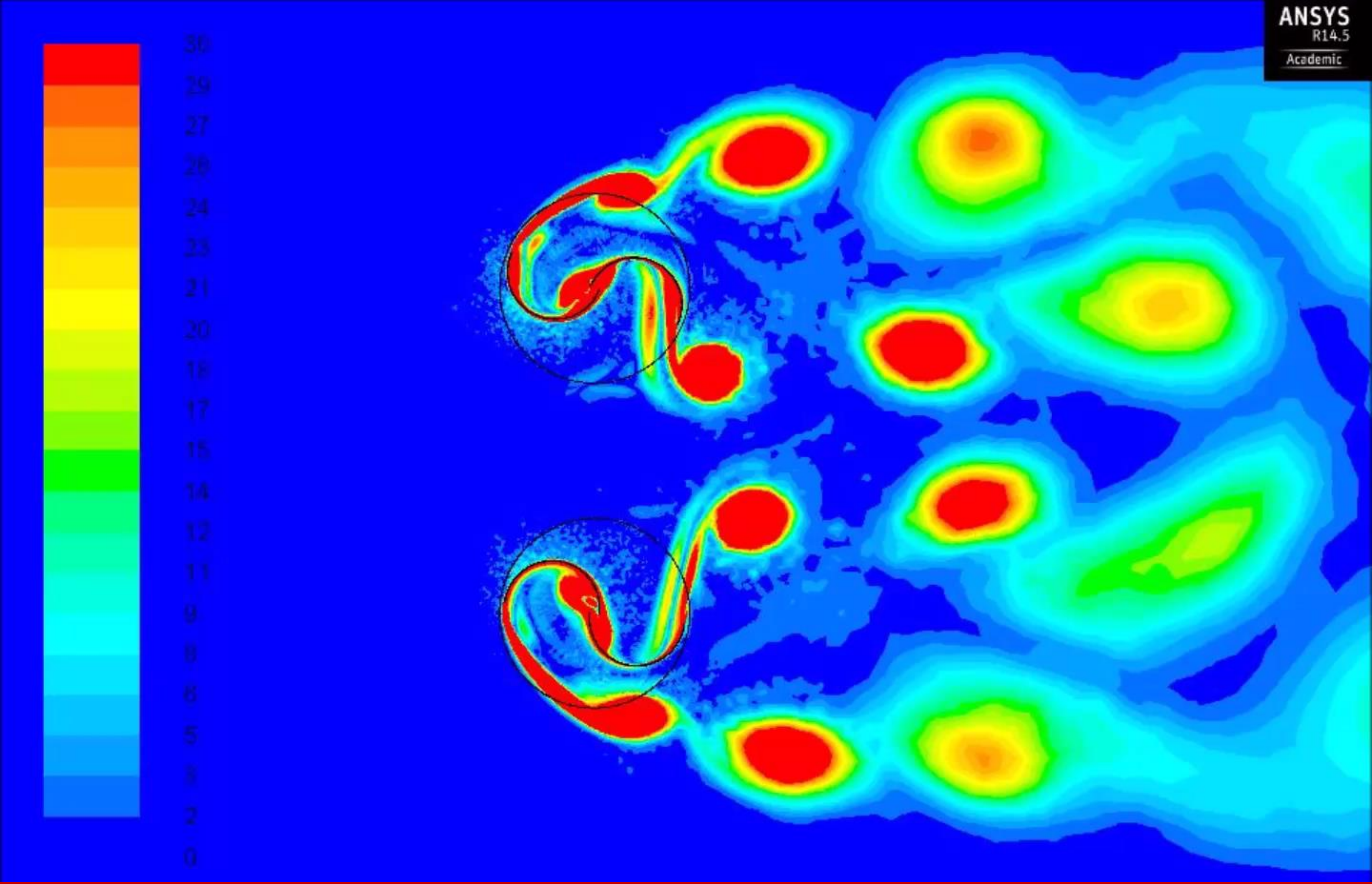

Vorticity Contours: Two Parallel Counter-Rotating Savonius Turbines

3- Two Oblique Co-Rotating Savonius Turbine Clusters

Case (A)

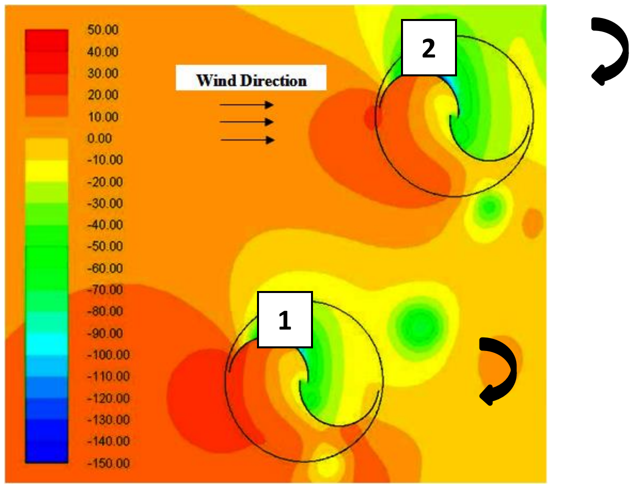

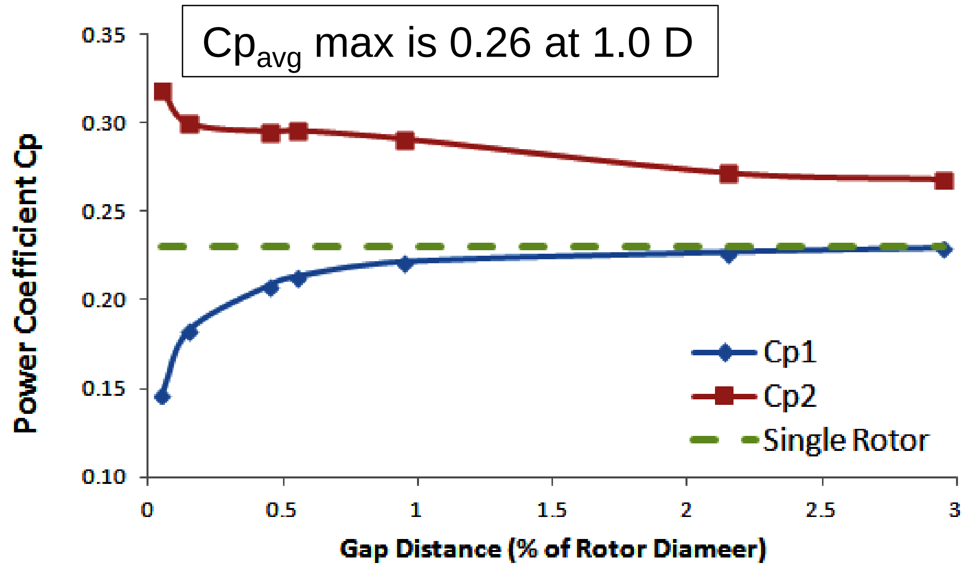

Case (B)

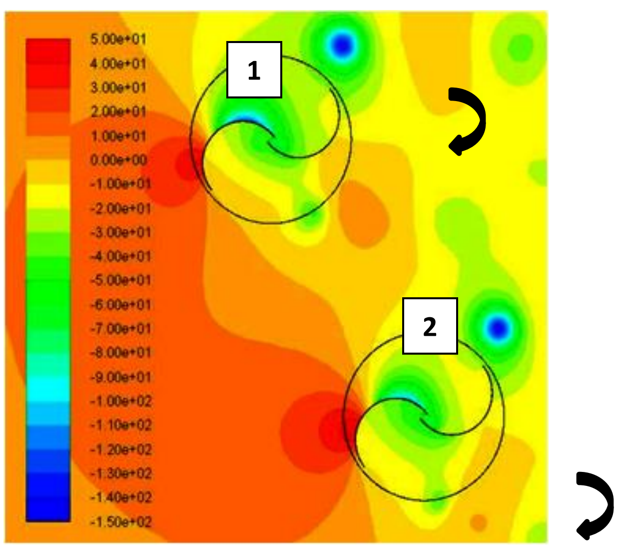

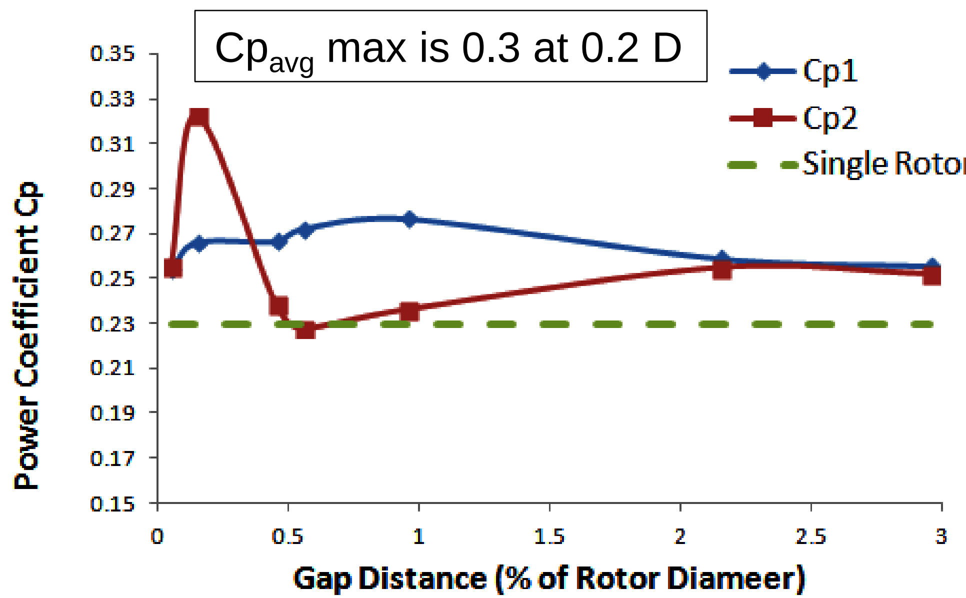

4- Two Oblique Counter-Rotating Savonius Turbine Clusters

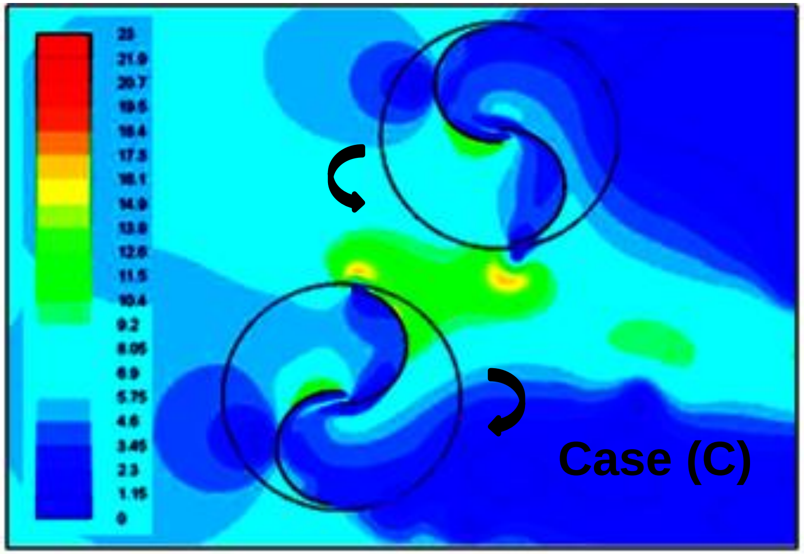

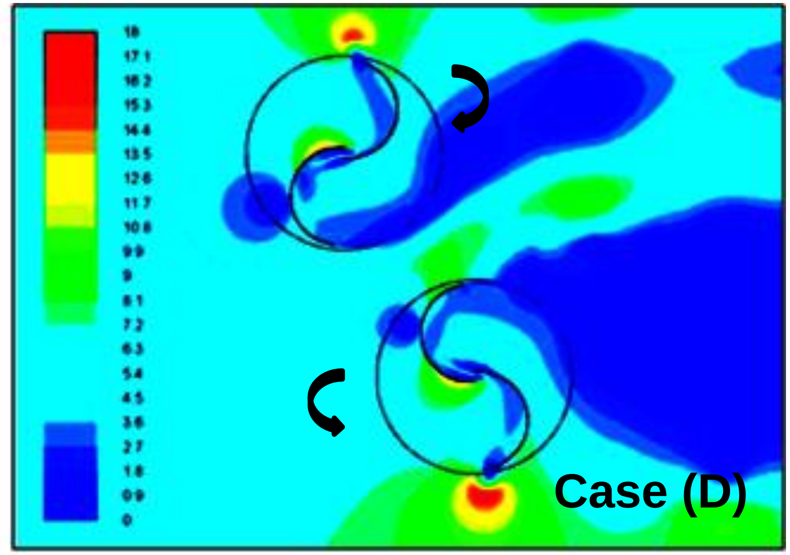

Cp_{avg} max is 0.35 at 0.4D

Cp_{avg} max is 0.25 at 1.6D

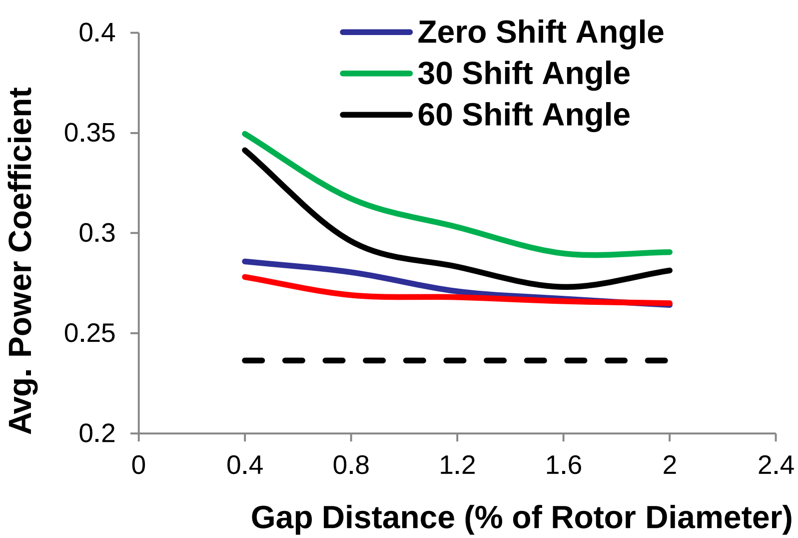

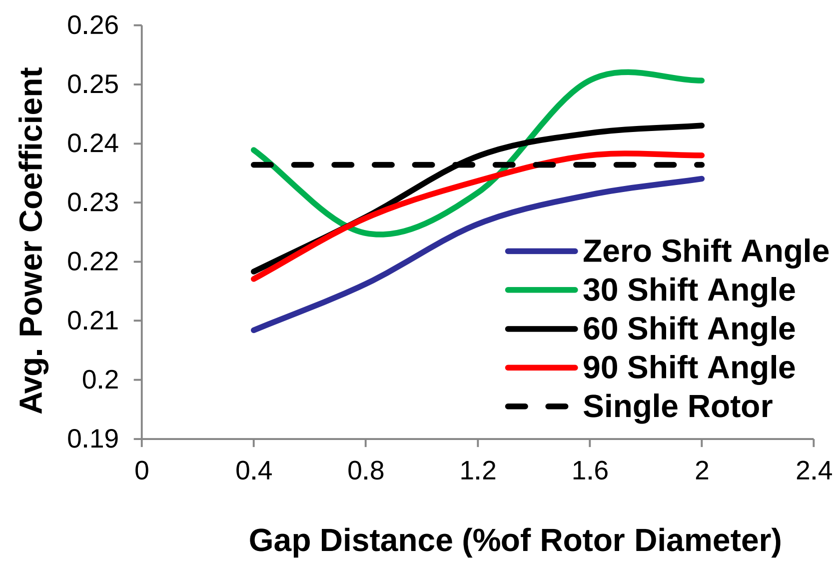

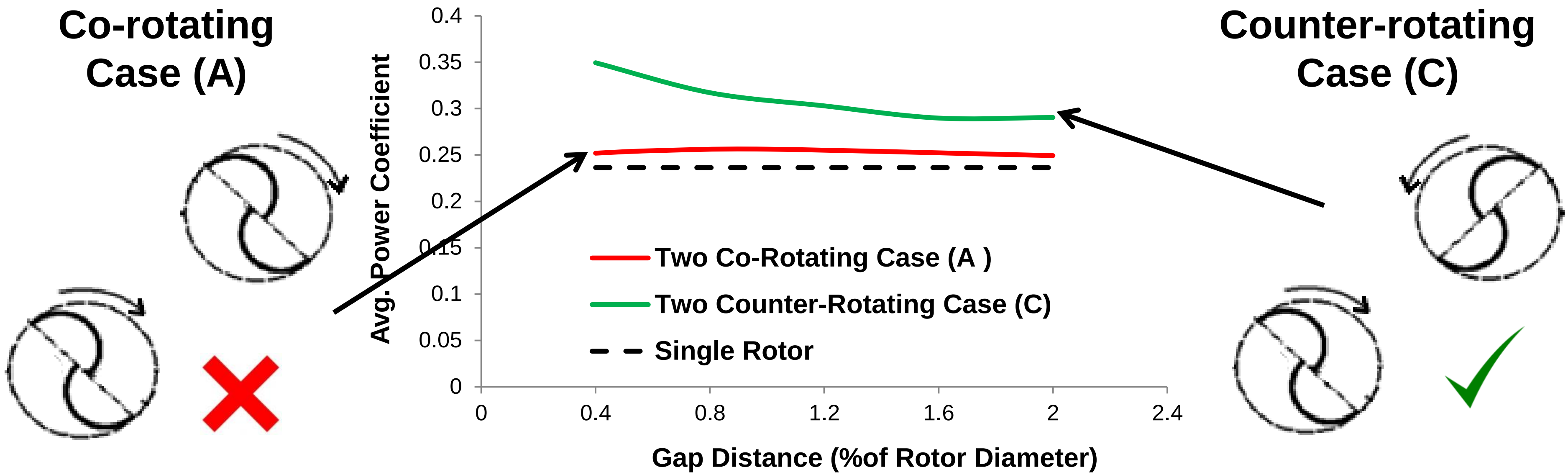
Co-rotating Case (A)
Counter-rotating Case (C)
Avg. Power Coefficient
0.4
0.35
0.3
0.25
0.2
0.15
0.1
0.05
0
0
0.4
0.8
1.2
1.6
2
2.4
Two Co-Rotating Case (A)
Two Counter-Rotating Case (C)
Single Rotor
Gap Distance (%of Rotor Diameter)

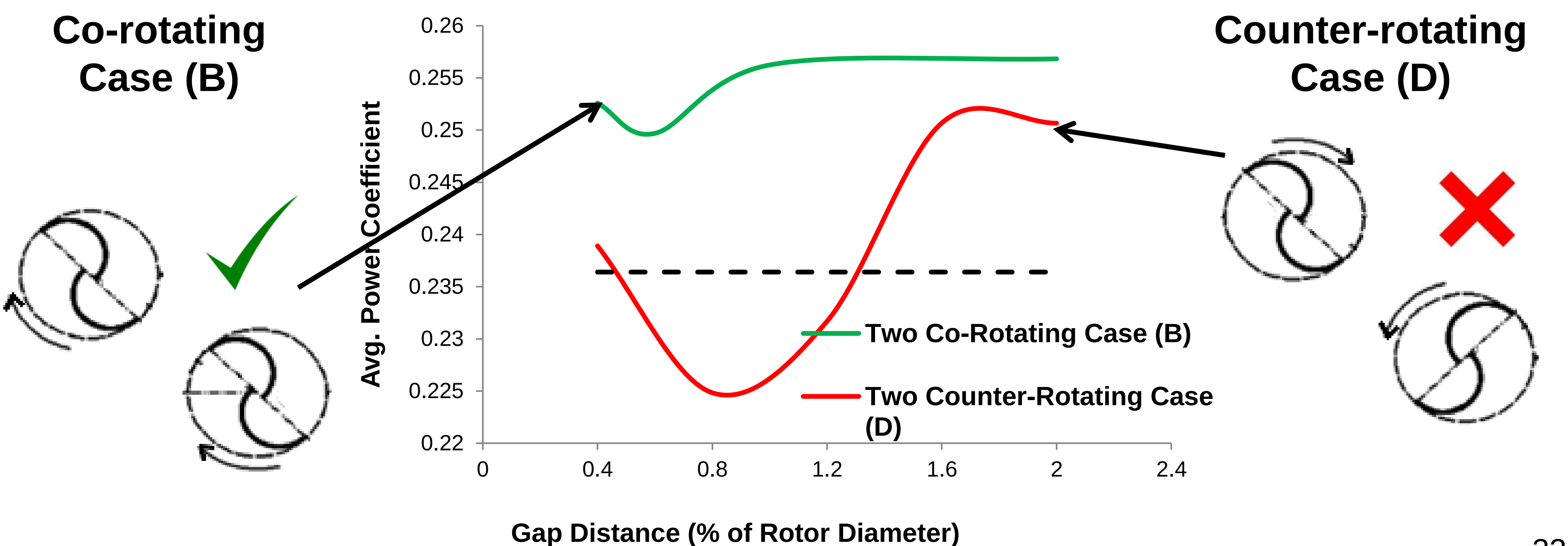
Co-rotating Case (B)
Counter-rotating Case (D)
Avg. Power Coefficient
0.26
0.255
0.25
0.245
0.24
0.235
0.23
0.225
0.22
0
0.4
0.8
1.2
1.6
2
2.4
Two Co-Rotating Case (B)
Two Counter-Rotating Case (D)
Gap Distance (% of Rotor Diameter)

Numerical Simulation of Three Turbine Savonius Clusters

Co-Rotating Cluster

Cp = 0.29

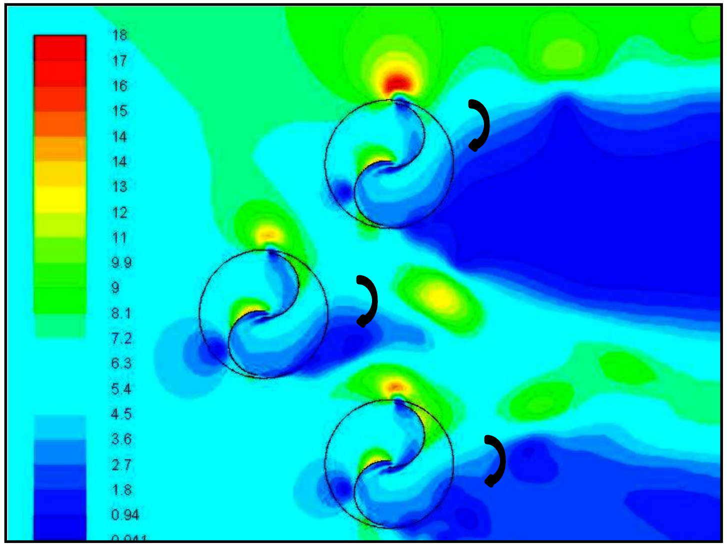

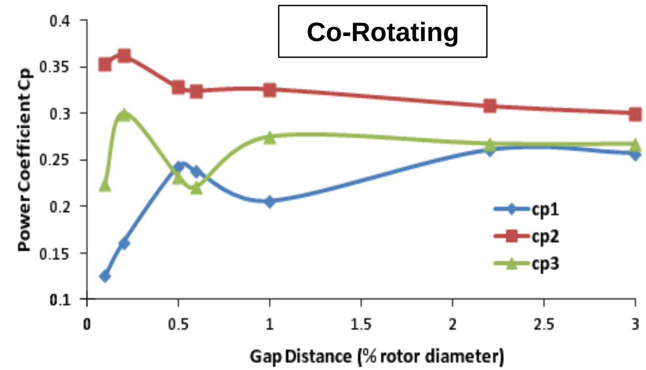

Hybrid Cluster

Cp=0.3

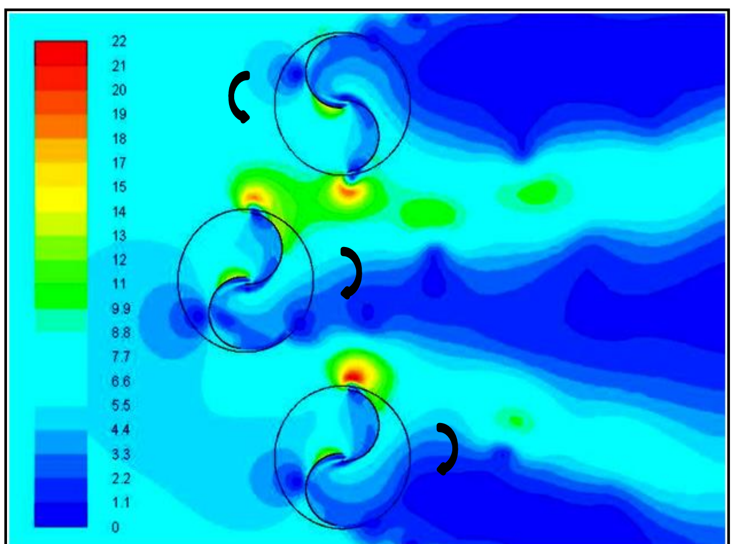

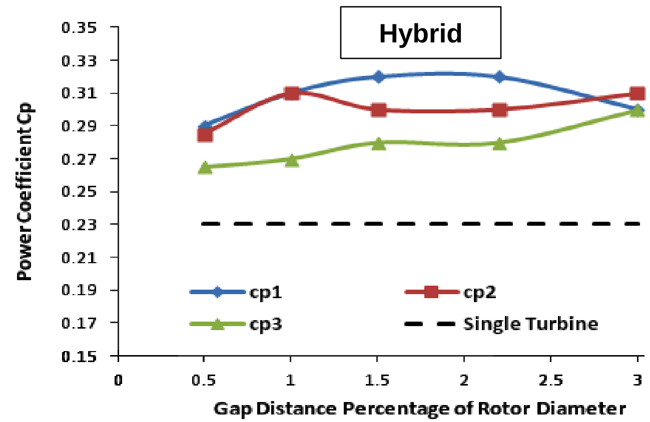

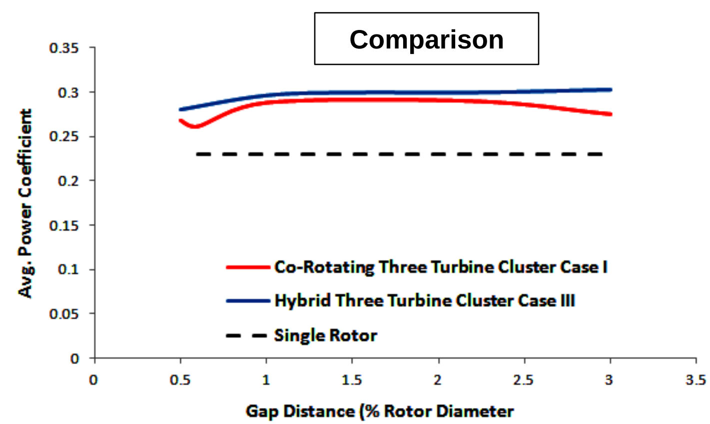

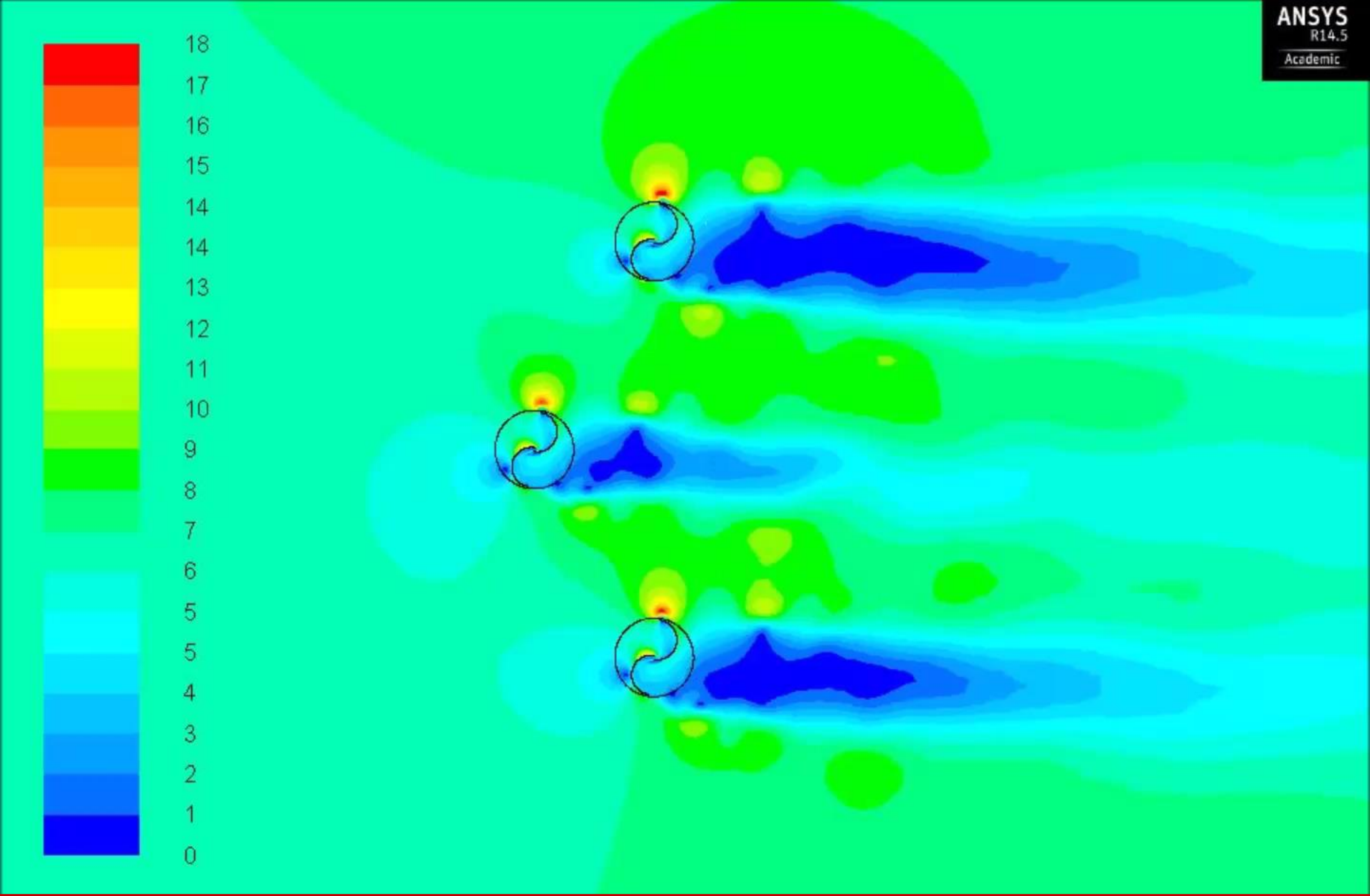

Velocity Contours: Three Co-Rotating Turbine Cluster

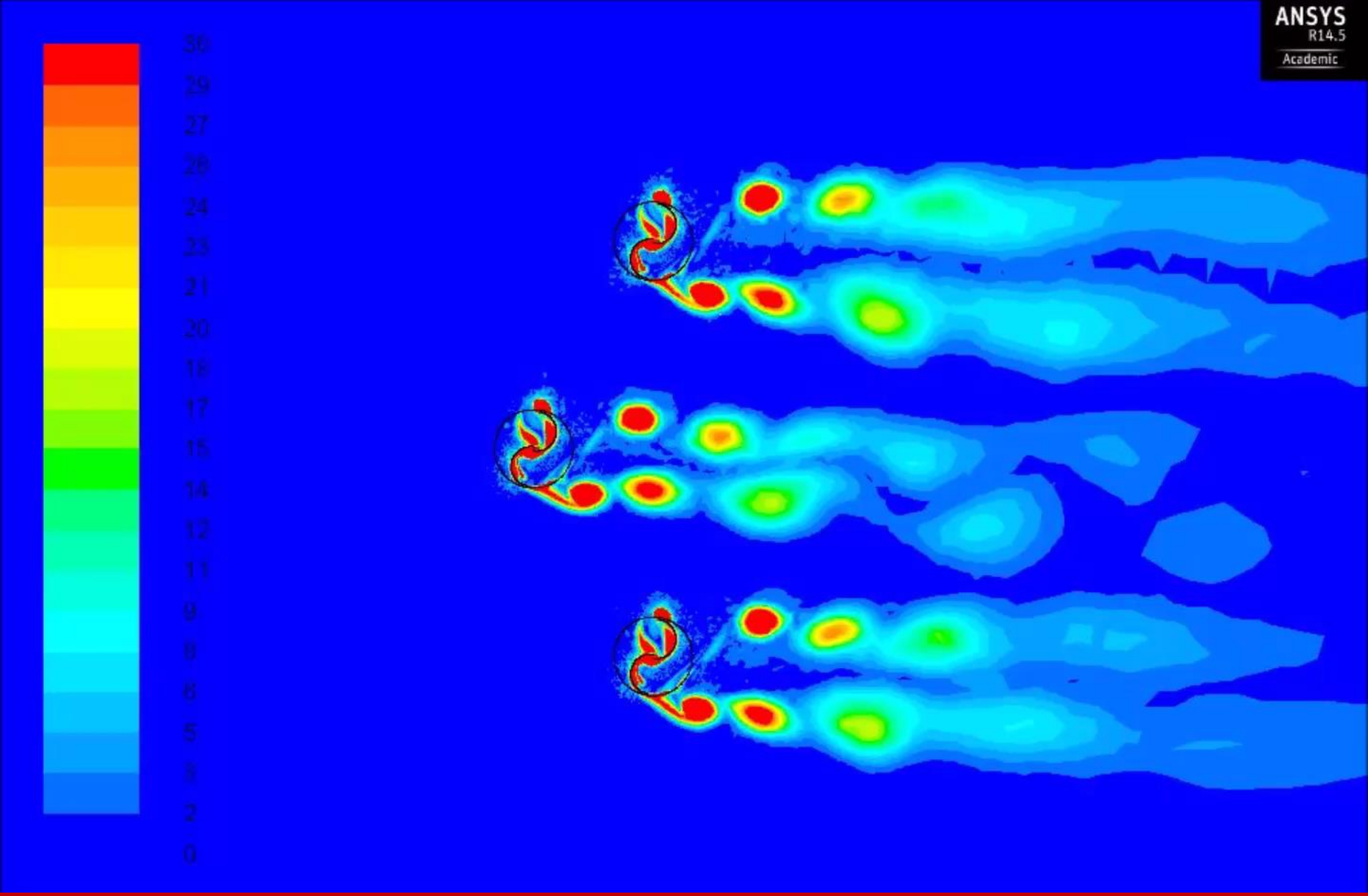

Vorticity Contours: Three Co-Rotating Turbine Cluster

Three Turbine Cluster Performance Confirmation

Co-Rotating Three turbine Cluster has an enhancement in average power coefficient of 26 % compared to isolated turbines

	Isolated Rotor	Rotor (1)	Rotor (2)	Rotor (3)
Power Coefficient (Cp)	0.23	0.26	0.327	0.289
Enhancement % Compared to Isolated Rotor		13%	42%	25%
Ratio Compared to Rotor (1)		1	1.23	1.07

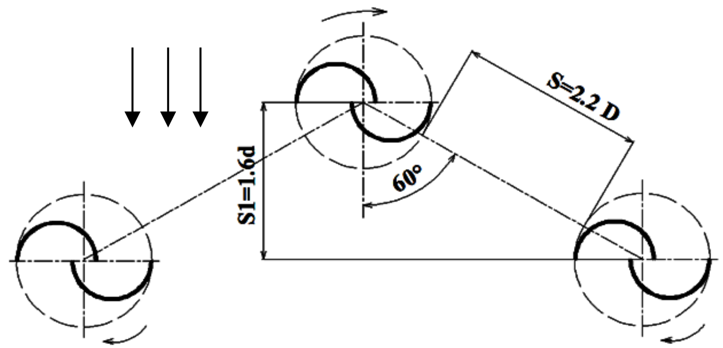

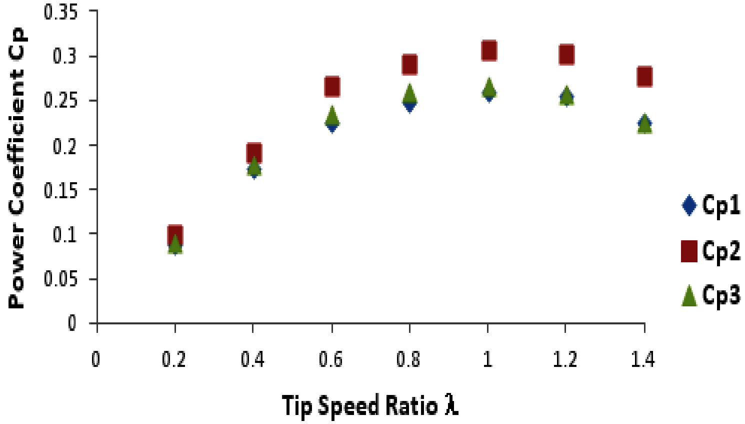

The results show that the ratio 1:1.2:1 between the power coefficients of the three rotors is consistent for $\lambda>0.6$

At $\lambda=1$, Cp_{max} = 0.286

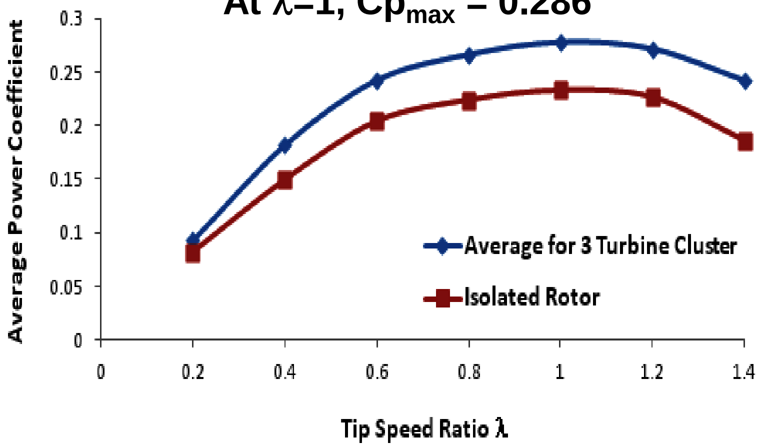

We focus here on the flow field at $\lambda>0.6$ in order to observe the flow-inducing action of the turbine revolutions rather than the flow-stagnating action at lower tip-speed ratios

Development of Patterned Savonius Wind Turbine Farms

- The efficient co-rotating three turbine cluster is used as a building unit for an efficient wind turbine farm

- Using the same triangular topology of the three turbine cluster the farm is developed as a geometric progression of the cluster

- Numerical simulations of farms that consist of nine and twenty-seven turbines are performed to confirm the pattern and the same enhancement ratio of the three turbine cluster and the geometric progression

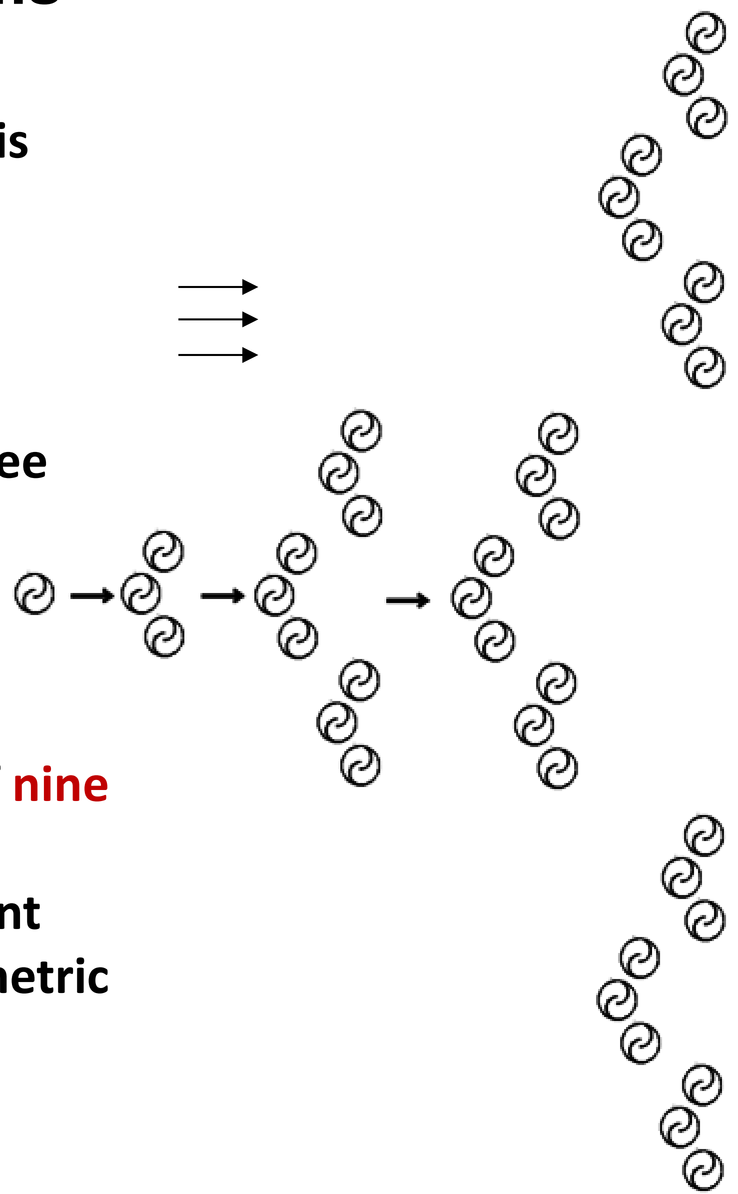

Development of Patterned Vertical Axis Wind Turbine Farm

Nine Savonius Wind Turbine Farm

The **nine turbine farm** is **triangular** and has the **same topology** of the three turbine **cluster**

Each vertex of the triangle has a **three turbine cluster**

The domain, solver setting and turbulence model are similar to that of the three turbine cluster simulation

The same grid topology is used, this results in a grid having a number of cells equal to 817,253 cells for the nine turbine farm simulation

The simulation time is about 32 hours

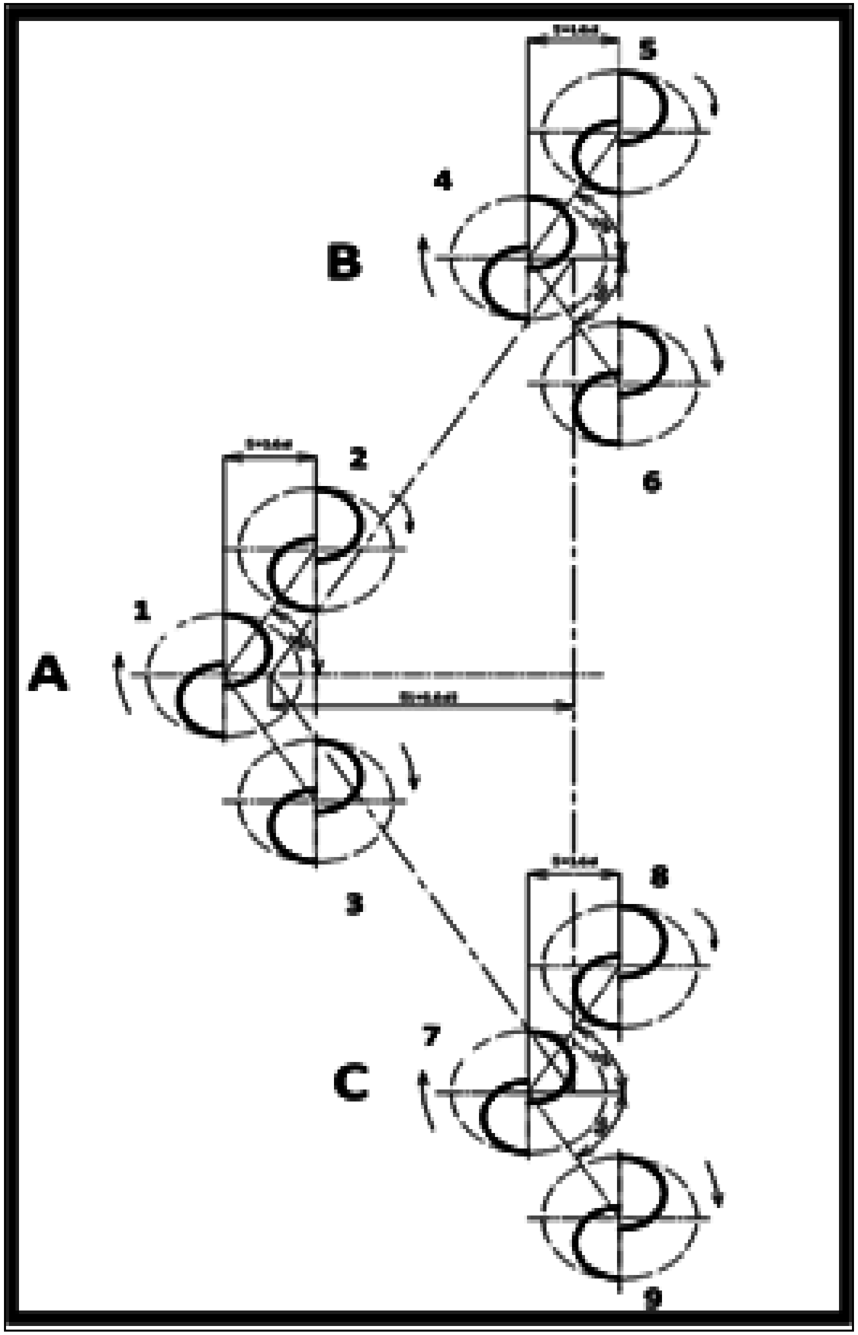

Numerical Results for the Nine Savonius Wind Turbine Farm

The ratio between Cp of the clusters (A:B:C) is 1:1.2:1

The ratio between Cp of individual turbines is (1:1.2:1)

The average power coefficient achieved by the developed nine turbine farm at λ=1 is 26% higher than that of isolated nine turbine farm

Cluster A	Isolated Rotor	Rotor (1)	Rotor (2)	Rotor (3)
Power Coefficient (Cp)	0.23	0.24	0.3	0.26
Enhancement % Compared to Isolated Rotor		4%	30%	13%
Ratio Compared to Rotor (1)		1	1.25	1.08
Cluster B	Isolated Rotor	Rotor (4)	Rotor (5)	Rotor (6)
Power Coefficient (Cp)	0.23	0.31	0.36	0.32
Enhancement % Compared to Isolated Rotor		34%	56%	39%
Ratio Compared to Rotor (4)		1	1.16	1.03
Cluster C	Isolated Rotor	Rotor (7)	Rotor (8)	Rotor (9)
Power Coefficient (Cp)	0.23	0.26	0.32	0.27
Enhancement % Compared to Isolated Rotor		13%	39%	17%
Ratio Compared to Rotor (7)		1	1.23	1.03

	Cluster (A)	Cluster (B)	Cluster (C)
Power Coefficient (Cp)	0.26	0.33	0.28
Ratio Compared to Cluster (A)	1	1.23	1.04

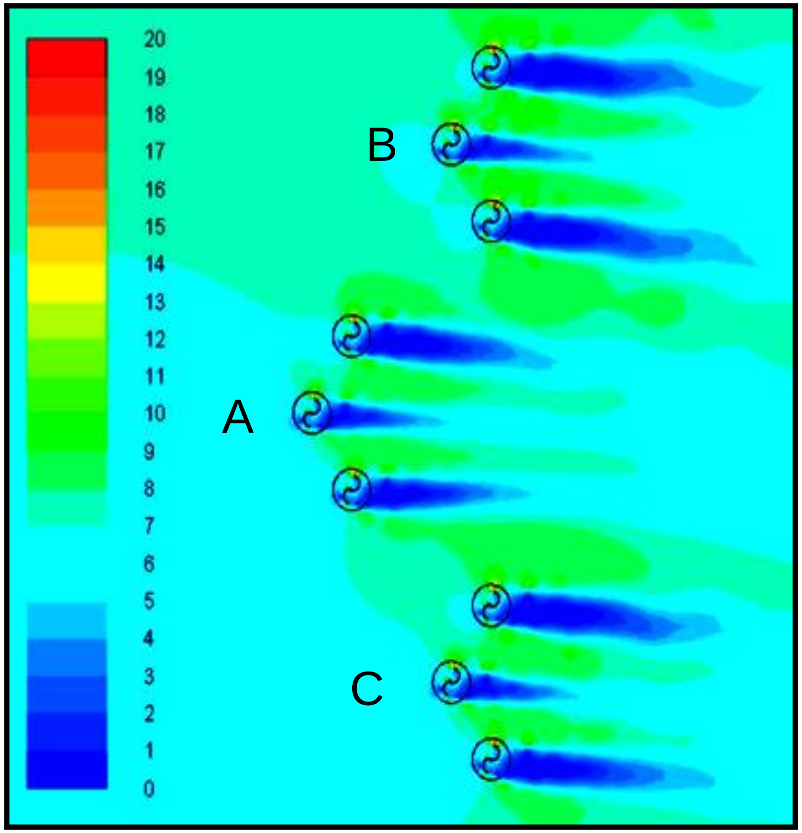

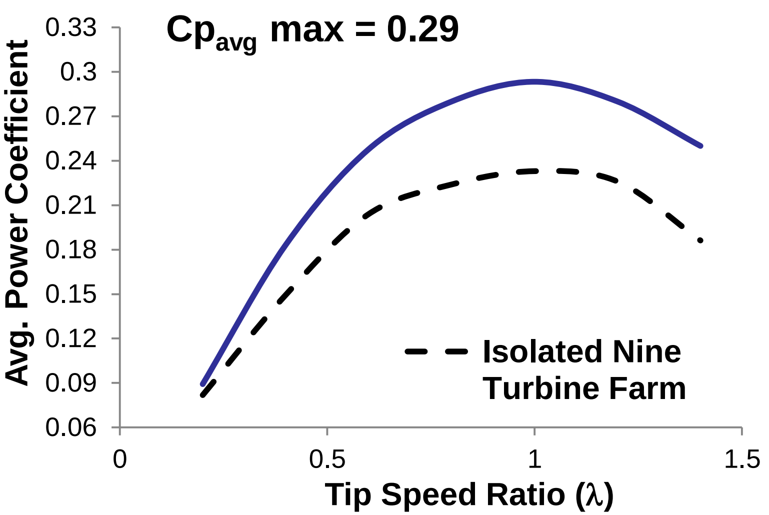

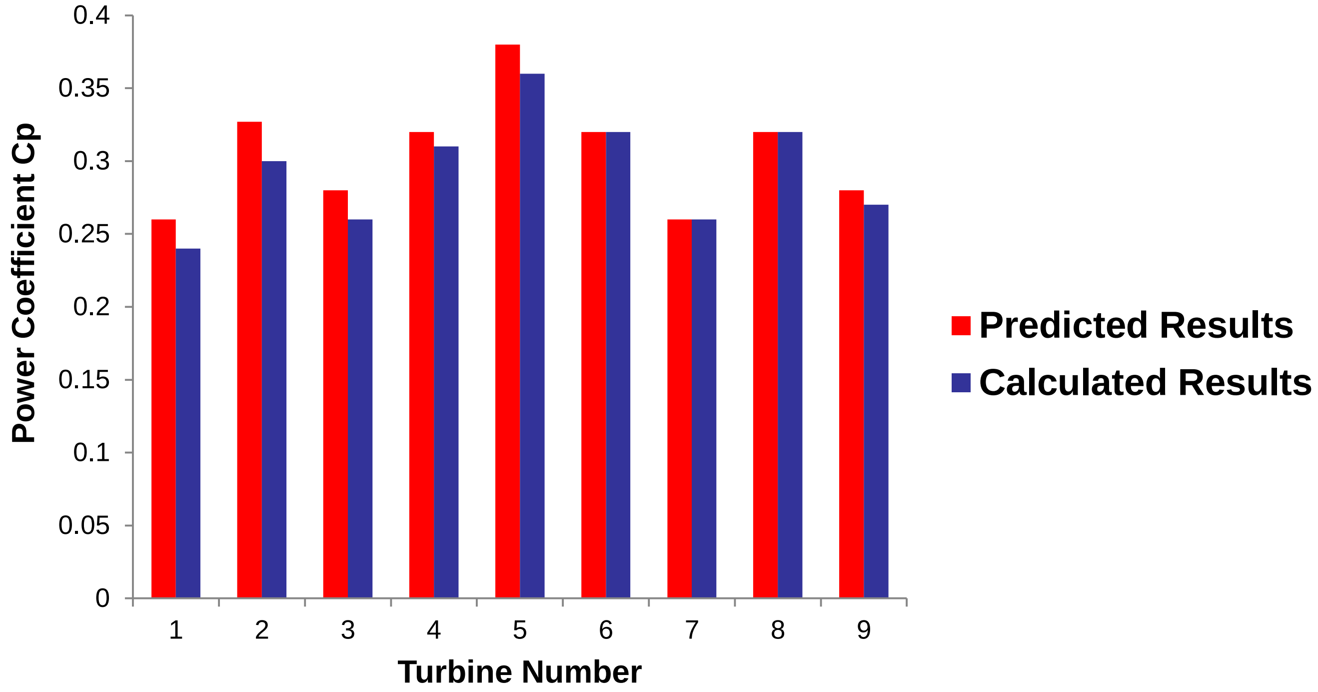

The nine turbine farm is patterned, the performance of the farm can be predicted by simulation of a three turbine cluster

Using the ratio 1:1.2:1 and the results of the three turbine cluster, the nine turbine farm efficiency is predicted and compared to the calculated results

The error in the predicted average power coefficient (Cp=0.3) of the farm compared to the calculated value (Cp=0.292) is less than 2%

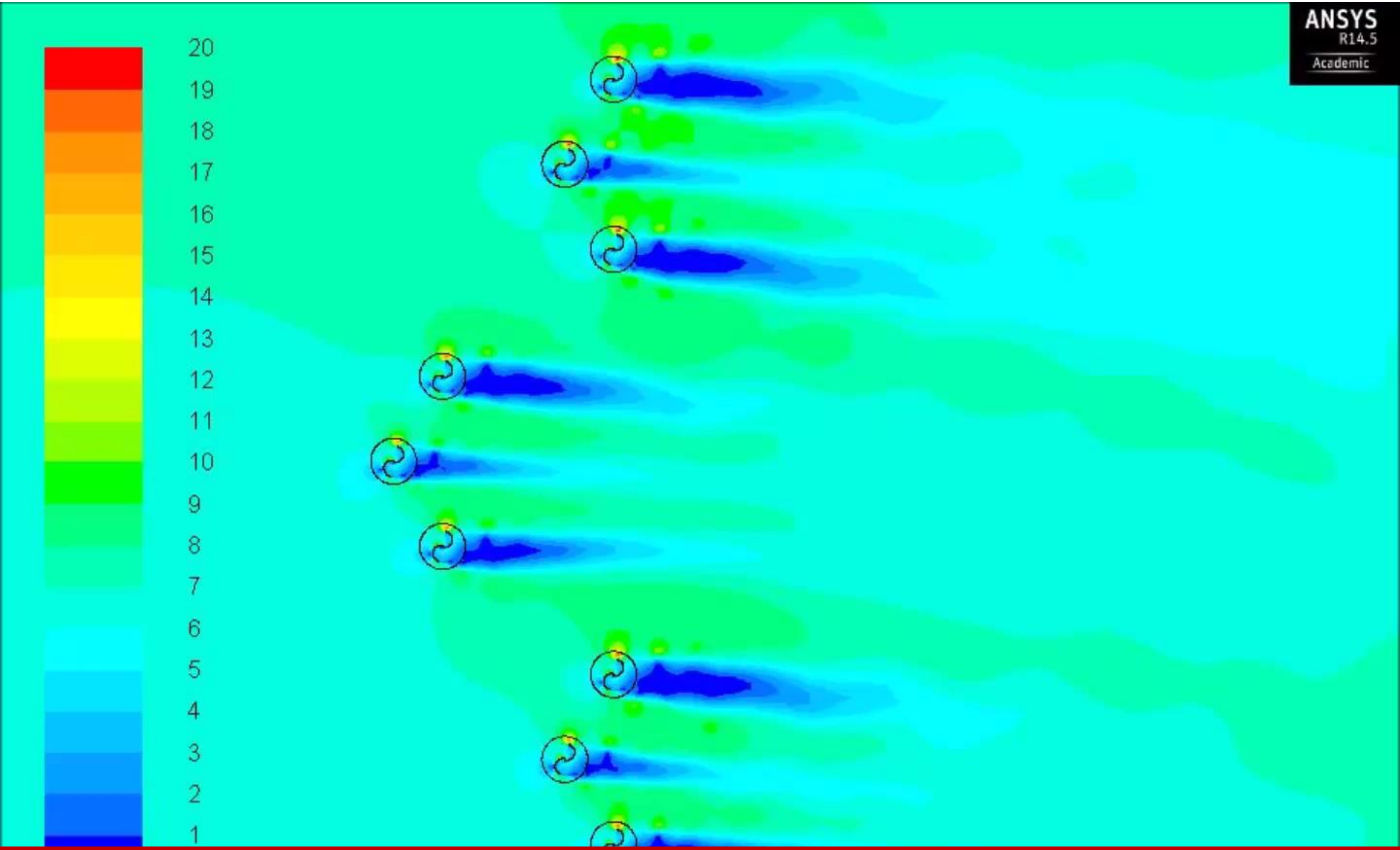

Velocity Contours: Co-Rotating Nine Savonius Turbine Farm

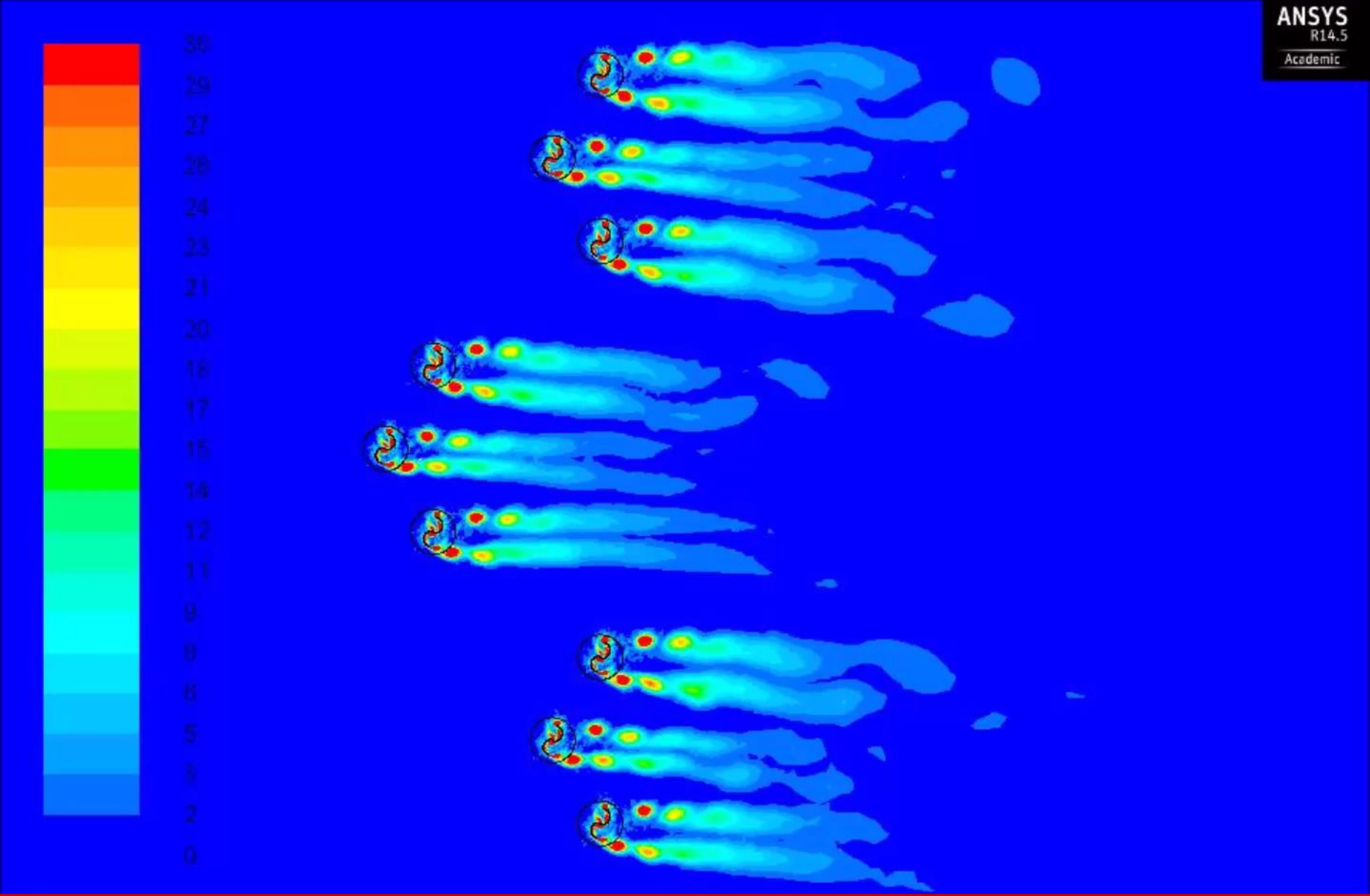

Vorticity Contours: Co-Rotating Nine Savonius Turbine Farm

Twenty Seven Savonius Wind Turbine Farm Simulation

The 27 turbine farm is **triangular** and has the **same topology** of the three turbine **cluster**

Each vertex of the triangle has a **nine turbine farm**

The domain, solver setting and turbulence model are similar to that of the three turbine cluster simulation

The same grid topology is used, this results in a grid having a number of cells equal to 2,751,759 cells for the 27 turbine farm simulation

The simulation time is about 120 hours

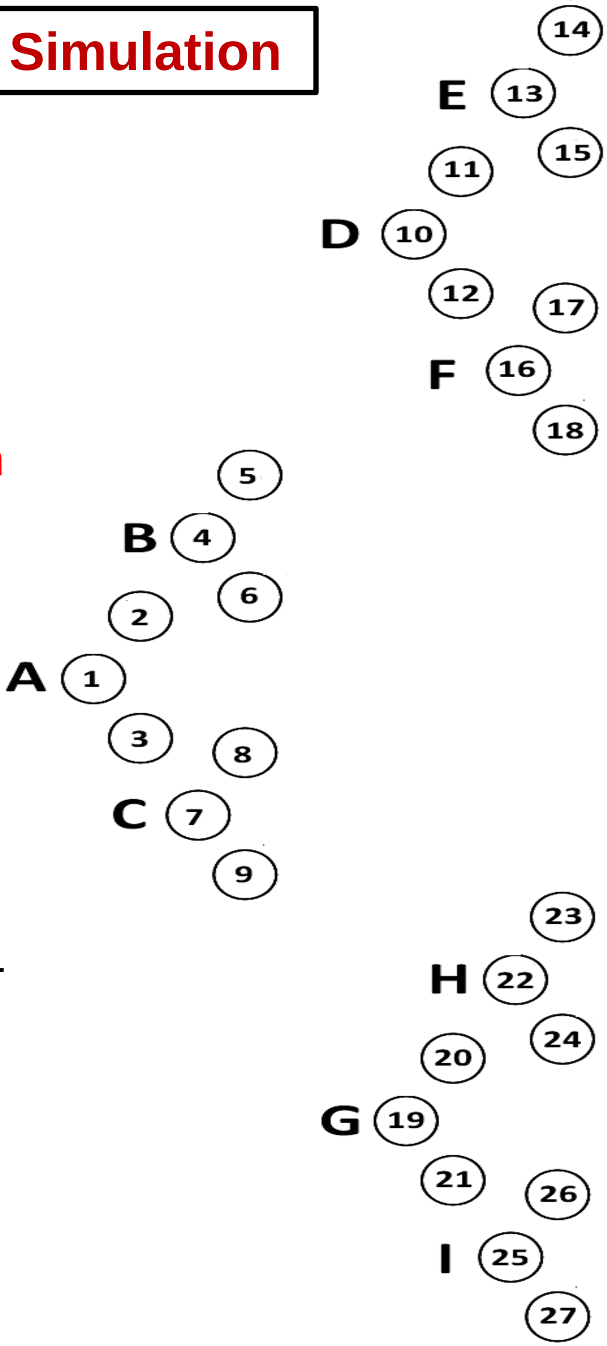

Numerical Results for the Twenty-Seven Savonius Wind Turbine Farm

The ratio between Cp of individual turbines is (1:1.2:1)

The ratio between average Cp of the clusters is 1:1.2:1

The ratio between average Cp of the nine turbine farms I, II and III is 1:1.2:1

The average power coefficient achieved by the developed nine turbine farms at λ=1 is 39% higher than that of isolated nine turbine farm

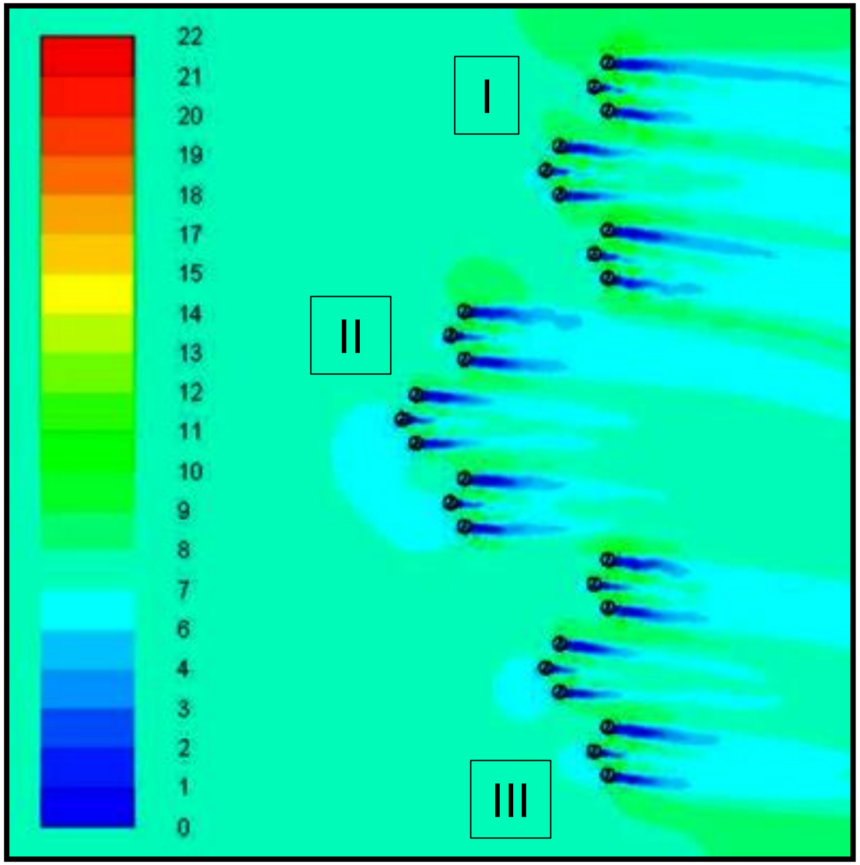

	Total Power (watt)	Ratio Compared to Cluster (A)
Cluster (A)	170	1
Cluster (B)	208	1.22
Cluster (C)	182	1.07
	Total Power (watt)	Ratio Compared to Cluster (D)
Cluster (D)	214	1
Cluster (E)	233	1.09
Cluster (F)	226	1.05
	Total Power (watt)	Ratio Compared to Cluster (A)
Cluster (G)	181	1
Cluster (H)	233	1.27
Cluster (I)	195	1.06

	Cluster (I)	Cluster (II)	Cluster (II)
Total Power (watt)	567	680	604
Ratio Compared to Cluster (I)	1	1.2	1.06

The average power achieved by the developed twenty-seven turbine farm is 0.32 at λ =1

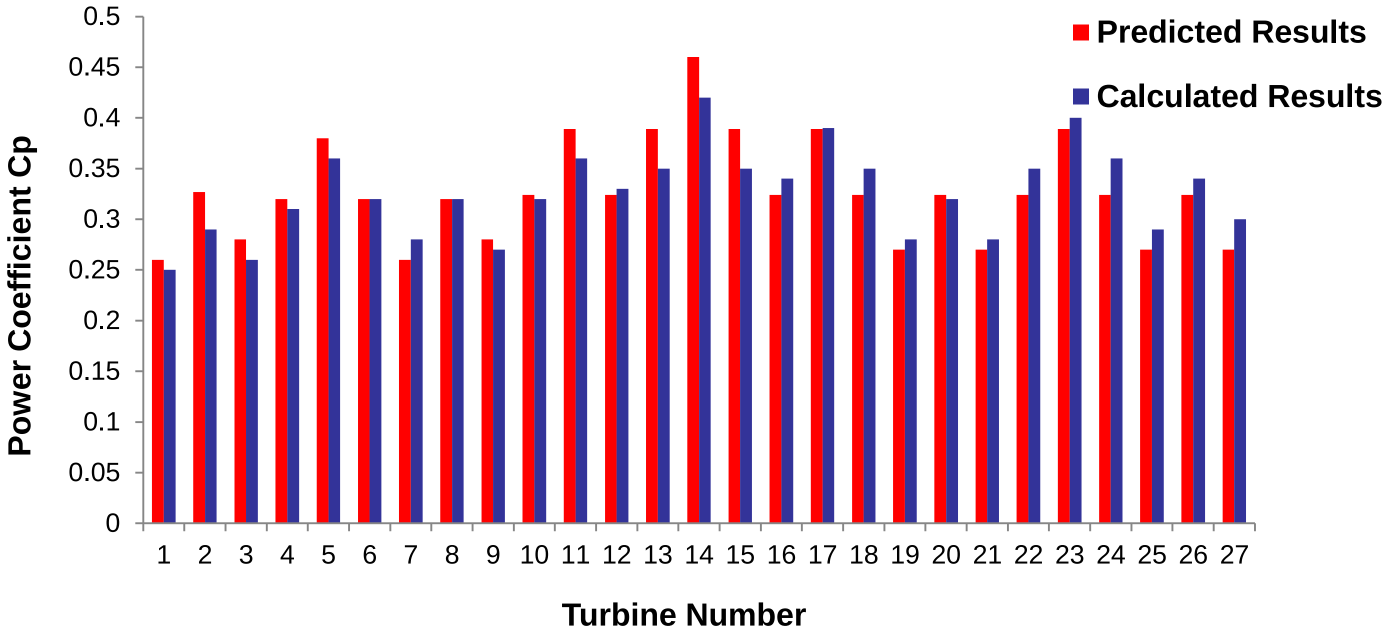

The 27 turbine farm is patterned, this means that the performance of the farm can be predicted by simulation of only three turbines.

Using the ratio 1:1.2:1 and the results of the simulation of the three turbine cluster, the 27 turbine farm efficiency is predicted and compared to the calculated results.

The error in the predicted average power coefficient (Cp=0.326) of the farm compared to the calculated value (Cp=0.325) is less than 0.4%

Power and Power Density of the Developed VS Isolated Farms (One meter Diameter and One meter Height Turbines)

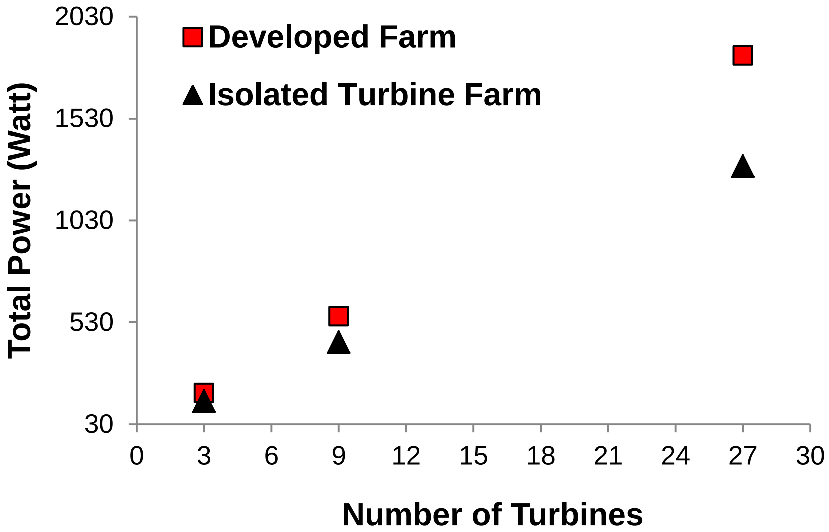

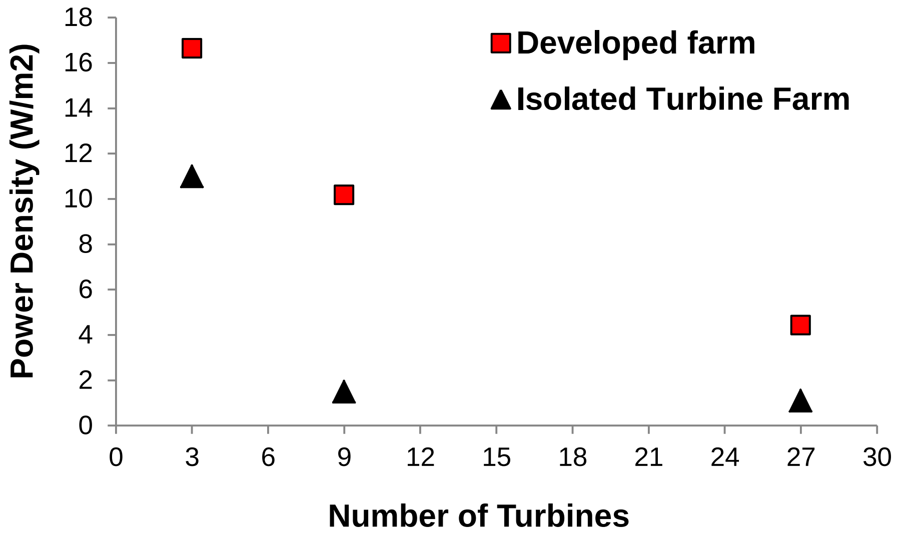

	Power (W/m)		Enhancement In Power	Power Density (W/m^2)		Enhancement In Power Density
	Developed	Isolated		Developed	Isolated	
3 Turbines	182	145	26%	17	13	1.3 times
9 Turbines	554	435	26%	10	1.9	7 times
27 Turbines	1841	1304	39%	4.5	1.5	4 times

Conclusion

- **Multiple Vertical axis wind Turbines arranged in closely configuration show enhancement in their performance compared to their isolated counter parts.**

- **The close arrangement enables to construct farms of higher power densities compared to conventional aligned isolated farms**

- **Two types of turbines VAWTS are numerically studied:**
  Savonius and Darrieus turbines

- **The enhanced performance is numerically studied for two parallel and oblique co-rotating and counter rotating configurations**

- **The numerical results are used to develop an efficient triangular three turbine cluster**

- **The performance of the Savonius three Turbine cluster is higher than three isolated turbines by 26% , and its power density is 1.5 times the isolated turbines at λ=1**

- **The performance of the Darrieus three Turbine cluster is higher than three isolated turbines by 30% , and its power density is 4 times the isolated turbines at λ=2.8**

- **The clusters performance is confirmed at different tip speed ratios, and the power ratio between the turbines is 1:1.2:1 for the Savonius cluster and 1:1.1:1 for the Darrieus cluster**

- **The efficient three turbine clusters are used to build efficient patterned Vertical axis wind turbine farms having the same geometric topology of the cluster and the same power ratio enhancement**

- **The pattern is confirmed by solving 9 and 27 Savonius turbine farms and a 9 turbine Darrieus farm**

- **The developed farms are patterned and have the same power ratios of the three turbine clusters**

- **The power density of the Savonius nine turbine farm is about 7 times a nine isolated turbine farm, and the power density of the twenty-seven turbine farm is 4 times a twenty-seven isolated turbine farm**

- **The power density of the Darrieus nine turbine farm is more than 13 times a nine isolated turbine farm**

- **The advantage of the patterned farm appears is the power ratio achieved by the clusters and confirmed by the farms**

- **This power ratio is used to predict the performance of larger farms with the same topology to save processing time and man power**

- **The developed farms have smaller structure size, wind farm signature, material and manufacturing costs than conventional HAWTs**

- **The developed farms are simpler in logistics of installation, operation and maintenance**

- **The developed farms are safer for birds, produce lower noise, and have a lower impact on radar signals**

- **A preliminary analysis of the mean velocity field around the turbine blades at different tip speed ratios shows a velocity distribution close to the structure of a Rankine vortex**

- **A future work will be considered for numerical modeling of the Darrieus turbine as a combination of the free stream with a Rankine vortex.**

- **The solution of adjacent vortices can be used to determine the performance of closely oriented Darrieus turbines and represented a farm by a group of vortices**

Summary of Savonius Turbine Clusters
(Single Turbine Cp= 0.23 at λ=1)

	Co-Rotating				Counter-Rotating					Farms	
	Two Turbines			Three Turbines	Two Turbines				Three Turbines	Nine Turbines	27 Turbines
	Parallel	Oblique			Parallel		Oblique				
		Case A	Case B		Case A	Case B	Case C	Case D			
Cp	0.3	0.26	0.32	0.29	0.26	0.3	0.35	0.25	0.3	0.3	0.32
Gap Distance	0.2D	1.0D	0.2D	2.2D	0.8D	0.8D	0.4D	1.6D	2.2D		

References

[1] Betz A. Introduction to the theory of flow machines. (D. G. Randall, Trans.). Oxford: Pergamon Press, 1966.

[2] World Wind Energy Association. 2014 half year report. August 2014.

[3] U.S. Department of Energy. 20% Wind Energy by 2030 - Increasing Wing Energy's Contribution to U.S. Electricity Supply. July 2008.

[4] MacKay D.J.C. Sustainable Energy—Without the Hot Air. UIT Cambridge Ltd., Cambridge, UK, 2009.

[5] John O. Dabiri. Potential order-of-magnitude enhancement of wind farm power density via counter-rotating vertical-axis wind turbine arrays. Journal Of Renewable And Sustainable Energy, 3: 043104, 2011.

[6] Robert W Whittlesey, Sebastian Liska and John O Dabiri. Fish schooling as a basis for vertical axis wind turbine farm design. Bioinspiration & biomimetics, 5: 035005, 2010.

[7] Lih-Shyng Shyu. A pilot study of vertical-axis turbine wind farm layout planning. Advanced Materials Research, 953-954: 395-399, 2014.

[8] R. Ganesh Rajagopalan, Ted L. Ricke. Aerodynamic interference of two vertical axis wind turbines. AIAA Applied Aerodynamics Conference; 6: 174-184, 1988.

[9] P.R. Schatzle, P.C. Klimas, and H.R. Spahr. Aerodynamic interference between two darrieus wind turbines. Journal of Energy, 5: 84-88, 1981.

[10] Zhou, T., Rempfer, D. Numerical study of detailed flow field and performance of Savonius wind turbines. Renewable Energy, 51: 373-381, 2013.

[11] Xiaojing, S., Daihai, L., Diangui, H., Guoqing, W. Numerical study on coupling effects among multiple Savonius turbines. Journal of Renewable and Sustainable Energy 4: 053107, 2012.

[12] Renewables 2014 Global Status Report "REN21".
[13] http://iipdigital.usembassy.gov/st/english/article/2013
[14] U.S. Department of Energy. 2013 Market report on wind technologies in distributed applications energy. Efficiency and Renewable Energy, 2014.
[15] The inside of a wind turbine. US Department of Energy, Office of Energy Efficiency & Renewable Energy, http://energy.gov/eere/wind/inside-wind-turbine-0
[16] Sandra Eriksson, Hans Bernhoff and Mats Leijon. Evaluation of different concepts for wind power, Renewable and Sustainable Energy, 12: 1419-1434, 2008.
[17] Windspire 1.2. Windspire Energy. Ark Alloy, LLC.
[18] Wikipedia the free encyclopedia. Savonius wind turbine, http://en.wikipedia.org/wiki/Savonius_wind_turbine
[19] R. Howell, N. Qin, J. Edwards, N. Durrani. Wind tunnel and numerical study of a small vertical axis wind turbine, Renewable Energy 35: 412–422, 2010.
[20] A. Shigetomi, Y. Murai, Y. Tasaka, Y. Takeda. Interactive flow field around two Savonius turbines, Renewable Energy, 36: 536-545, 2011.
[21] R. E. Sheldahl, B. F. Blackwell, and L. V. Feltz. Wind tunnel performance data for two- and three-bucket Savonius rotors, Sandia Report, SAND 77-0131, 1977.
[22] B. D. Altan, M. Atilgan, and A. Ozdamar. An experimental study on improvement of a Savonius rotor performance with curtaining, Exp. Therm. Fluid Sci. 32(8): 1673–1678, 2008.
[23] B. Kirke. Development in ducted water current turbines, www.Cyberiad.net.
[24] N. Fujisawa. On the torque mechanism of Savonius rotors, J. Wind Eng. Ind. Aerodyn. 40(2): 277–292, 1992.
[25] Dixon, K. R. The Near Wake Structure of a Vertical Axis Wind Turbine. Thesis. Delft University of Technology, 2008.

[26] Tong, Wei. Wind Power Generation and Wind Turbine Design. Southampton: WIT, 2010.
[27] K. Pope, G.F. Naterer, I. Dincer and E. Tsang. Power correlation for vertical axis wind turbines with varying geometries, International Journal Of Energy Research, 35: 423–435, 2011.
[28] H. Riegler. HAWT Versus VAST Small VAWTs Find a Clear Niche. Refocus 4: 44–46, 2003.
[29] http://www.windturbine-analysis.netfirms.com
[30] D'Ambrosio M., Medaglia M. Vertical Axis Wind Turbines: History, Technology and Applications: Master thesis, (2010).
[31] Ajedegba J.O. Effect of Blade Configuration on Flow Distribution and Power Output of a Zephir Vertical Axis Wind Turbine, University of Ontario Institute of Technology: Master thesis, 2008.
[32] Shepherd W., Zhang L., Electricity Generation using Wind Power, World scientific, 2011.
[33] Yaoa. J, Wanga J., Yuanb W., Wanga H. & Caoa L. Analysis on the influence of Turbulence model changes to aerodynamic performance of vertical axis wind turbine, International Conference on Advances in Computational Modeling and Simulation, 31: 213-219, 2011
[34] K. N. Morshed, M. Rahman, G. Molina and M. Ahmed. Wind tunnel testing and numerical simulation on aerodynamic performance of a three-bladed Savonius wind turbine, International Journal of Energy and Environmental Engineering, 4-18, 2013.
[35] Uzarraga-Rodriguez N. Cristobal, Gallegos-Muñoz A. and Riesco Ávila J. Manuel. Numerical Analysis of A Rooftop Vertical Axis Wind Turbine, International Conference on Energy Sustainability, ES2011-54173, 2011.

[36] K. Kacprzak, G. Liskiewicz, K. Sobczak. Numerical investigation of conventional and modified Savonius wind turbines, Renewable Energy, 60: 578-585, 2013.
[37] M.H Mohamed, G. Janiga, E. Pap, D. Thévenin. Optimal Blade Shape of a Modified Savonius Turbine using an Obstacle Shielding the Returning Blade, Energy Conversion and Management 52(1): 236-242, 2011.
[38] R. Lanzafame, S. Mauro, M. Messina, " 2D CFD Modeling of H-Darrieus Wind Turbines using a Transition Turbulence Model," Energy Procedia 45 (2014) 131–140
[39] F. R. Menter, "Two Equation Eddy Viscosity Turbulence Models for Engineering Applications," AIAA Journal Vol. 32, No. 8, August 1994.
[40] Langtry R.B., Menter F.R., Likki S.R., Suzen Y.B., Huang P.G., Völker S. A correlation based transition model using local variables part I: model formulation, ASME GT 2004 - 53452, 2006
[41] McLaren KW. A numerical and experimental study of unsteady loading of high solidity vertical axis wind turbines, McMaster: McMaster University, 2011. Open Access Dissertations and Theses Paper 6091. http://digitalcommons.mcmaster.ca/opendissertations
[42] J. M. Edwards, L. A. Danao and R. J. Howell. Novel Experimental Power Curve Determination and Computational Methods for the Performance Analysis of Vertical Axis Wind Turbines, Journal of Solar Energy Engineering, 134: 031008-1, 2012.
[43] M. Nakajima, S. IIO and T. Ikeda. Performance of Double-step Savonius Rotor for Environmentally Friendly Hydraulic Turbine, Journal of Fluid Science and Technology 3, 2008.
[44] N. Fujisawa and F. Gotoh. Visualization study of the flow in and around a Savonius rotor, Experiments in Fluids, 12: 407-412, 1992.
[45] Ivan Dobrev, Fawaz Massouh. CFD and PIV investigation of unsteady flow through Savonius wind turbine, Energy Procedia, 6:711–720, 2011.

[46] Zullah M.A, Prasad D, Choi Y.D, Lee Y.H. Study on the performance of helical Savonius rotor for wave energy conversion, AIP Conf. Proc,1225: 641-649, 2010.
[47] Kang, C., Zhang, F., Mao, X. Comparison study of a vertical-axis spiral rotor and a conventional Savonius rotor, *APPEEC*, Art. No. 5448791, 2010.
[48] Yaakob O.B, Tawi, K.B, Sunanto, D.T.S. Computer Simulation Studies on the effect overlap ratio for Savonius type vertical axis marine current turbine, " *Int. J. of Eng., Trans. A*: Basics, 23(1): 79-88, 2010.
[49] J. V. Akwaa,H. A. Vielmob, A. P. Petry. A Review on The Performance of Savonius Wind Turbines, *Renewable and Sustainable Energy Reviews*, 16: 3054 – 3064, 2012.
[50] Taher G. Abu-El-Yazied, Hossam N. Doghiem, Ahmad M. Ali, and Islam M. Hassan," Investigation of the Aerodynamic Performance of Darrieus Vertical Axis Wind Turbine," IOSR Journal of Engineering (2014) 4: 18-29
[51] R. Lanzafame, S. Mauro, M. Messina, " 2D CFD Modeling of H-Darrieus Wind Turbines using a Transition Turbulence Model," Energy Procedia (2014) 45: 131 – 140
[52] E. Amet, T. Maitre, C. Pellone, J. L. Achard " 2D Numerical Simulations of Blade-Vortex Interaction in a Darrieus Turbine," Journal of Fluids Engineering (2009) 131: 111103-1
[53] Lanzafame R., Mauro S., Messina M. Wind turbine CFD modeling using a correlation-based transitional model. Renewable Energy 52 (2013) 31 - 39
[54] K. Kacprzak, G. Liskiewicz, K. Sobczak, " Numerical investigation of conventional and modified Savonius wind turbines," Renewable Energy (2013) 60: 578-585
[55] I. Paraschivoiu, " Wind Turbine Design With Emphasis on Darrieus Concept," Polytechnic, Brooklyn, NY, (2002).

[56] J.H. Strickland, B.T. Webster, and T. Nguyen, “A Vortex Model of the Darrieus Turbine: An Analytical and Experimental Study,” American Society of Mechanical Engineers (1979) 79- WA/FE-6.
[57] R. Rajagopalan and T. Rickerl, “Aerodynamic Interference of Vertical Axis Wind Turbines,” Journal of Propulsion (1990) 6: 645-653
[58] Kailash Golecha, T. I. Eldho, and S. V. Prabhu , “ Study on the Interaction between Two Hydrokinetic Savonius Turbines”, International Journal of Rotating Machinery (2012) Article ID 581658

Publications

<u>Published Journal Papers:</u>

- M. Shaheen , M. El-Sayed, and Shaaban Abdallah, “**Numerical Study of Two-Bucket Savonius Wind Turbine Cluster**” Journal of Wind Engineering & Industrial Aerodynamics.

Reviewers Comments:

In fact, the reviewer acknowledges the authors for doing very well in the manuscript.

Without any doubt, the authors tackle a highly interesting problem in the field of VAWTs and the numerical approach sounds extremely inviting.

It is my impression that this is a well written paper and is of a quality/standard worth publishing

Bending Journal and Conference Papers

- M. Shaheen and Shaaban Abdallah, "Efficient Clusters and Patterned Farms for Darrieus Wind Turbines ," Journal of Renewable Energy
- M. Shaheen and Shaaban Abdallah, " Development of Efficient Savonius Vertical Axis Wind Turbine Clustered Farms ," Journal of Sustainable Energy
- M. Shaheen and Shaaban Abdallah, "A Numerical Comparison Study between Co-Rotating and Counter-Rotating Savonius Wind Turbine Clusters " 3rd International Conference and Exhibition on Mechanical & Aerospace Engineering 2015, US, Los Angeles

Poster Presentation:

- M. Shaheen , M. El-Sayed, and Shaaban Abdallah, "**Numerical Study of Two-Bucket Savonius Wind Turbine Cluster**," 2nd International Conference and Exhibition on Mechanical & Aerospace Engineering. September 08-10, 2014 Philadelphia, USA
- M. Shaheen , and Shaaban Abdallah, " **A Novel Clustered and Patterned Vertical axis Wind Turbine Farm** ," Graduate Student Expo & Poster Forum 2015, University of Cincinnati.

Under Construction

- " **Physical Insights for vortex modeling of Darrieus Vertical Axis Wind Turbines**"

Awards

- "**Award for Exemplary Poster Presentation in the Category of Physical Science and Engineering**," Graduate Student Expo & Poster Forum 2015, University of Cincinnati.

- "**R. T. Davis Award , A Graduate Student with Demonstrated Aptitude and Scholar ship in the Field of Computational Mechanics**,". University of Cincinnati, Department of Aerospace Engineering and Engineering Mechanics.

Acknowledgment

- Professor **Shaaban Abdallah**:
  - For his guidance and all the useful discussions and brainstorming sessions
  - His understanding and support

- **Committee members** for their friendly meetings and encouraging precious insights and suggestions

- Department of Aerospace Engineering and Engineering Mechanics

- PhD students

- My **father and mother** who gave me the dream since I have been a child

- My kids **Nourhan**, **Youssef** and **Kareem** for their constant unconditional emotional support

- My wife **Walaa Mazhar**, She has been a constant source of strength and inspiration


Thank you!


Questions

Force Analysis on Darrieus Turbine

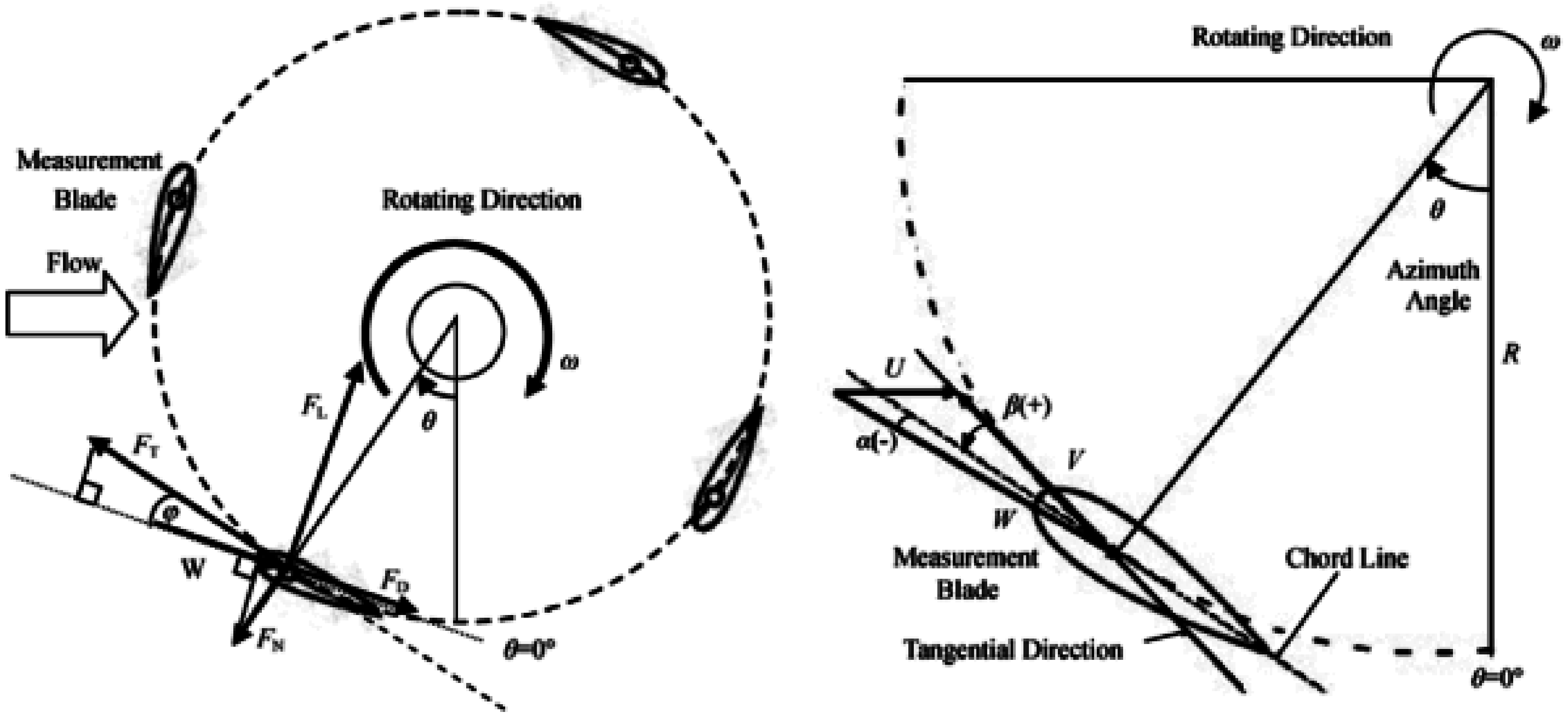

Variation in Angle of Attack Vs Tip Speed Ratio

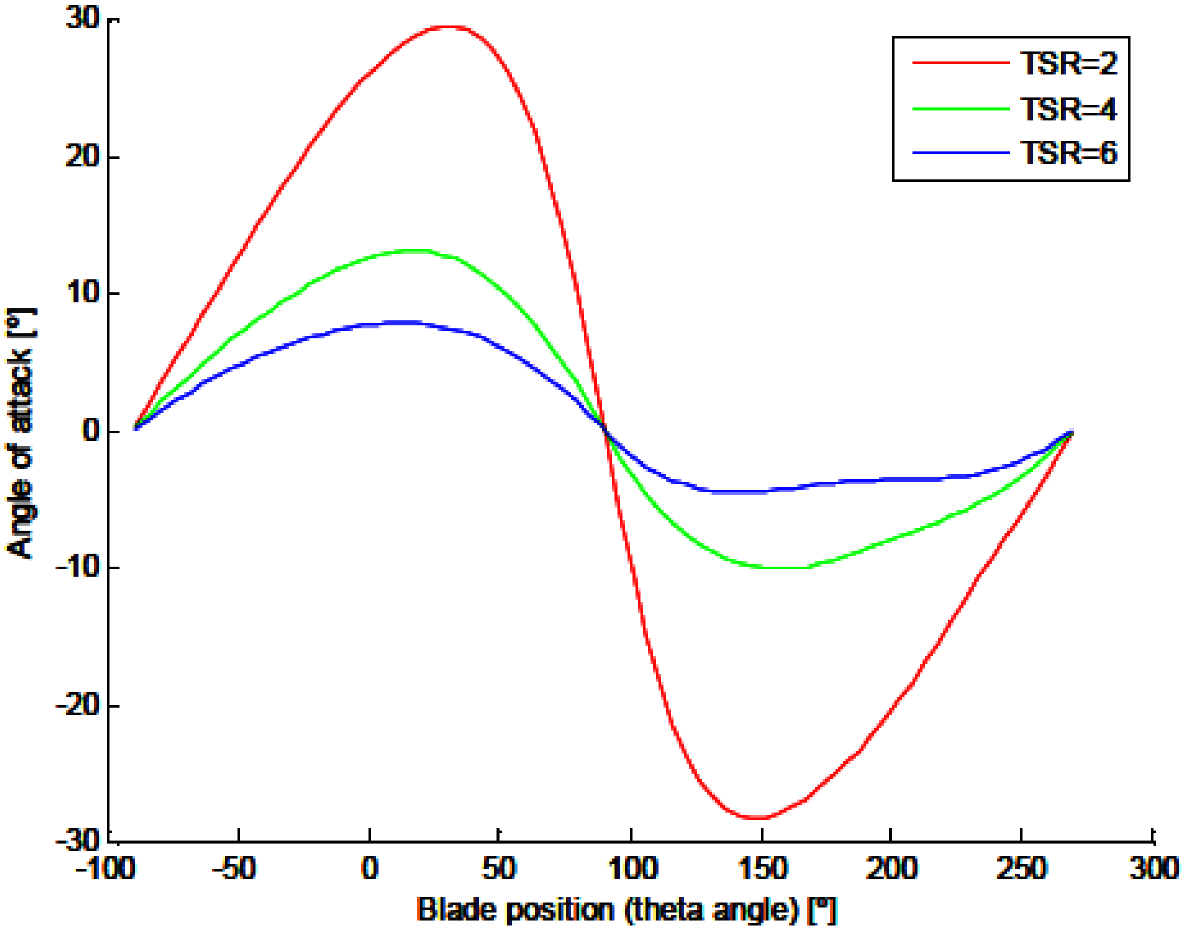

Transition in VAWTs

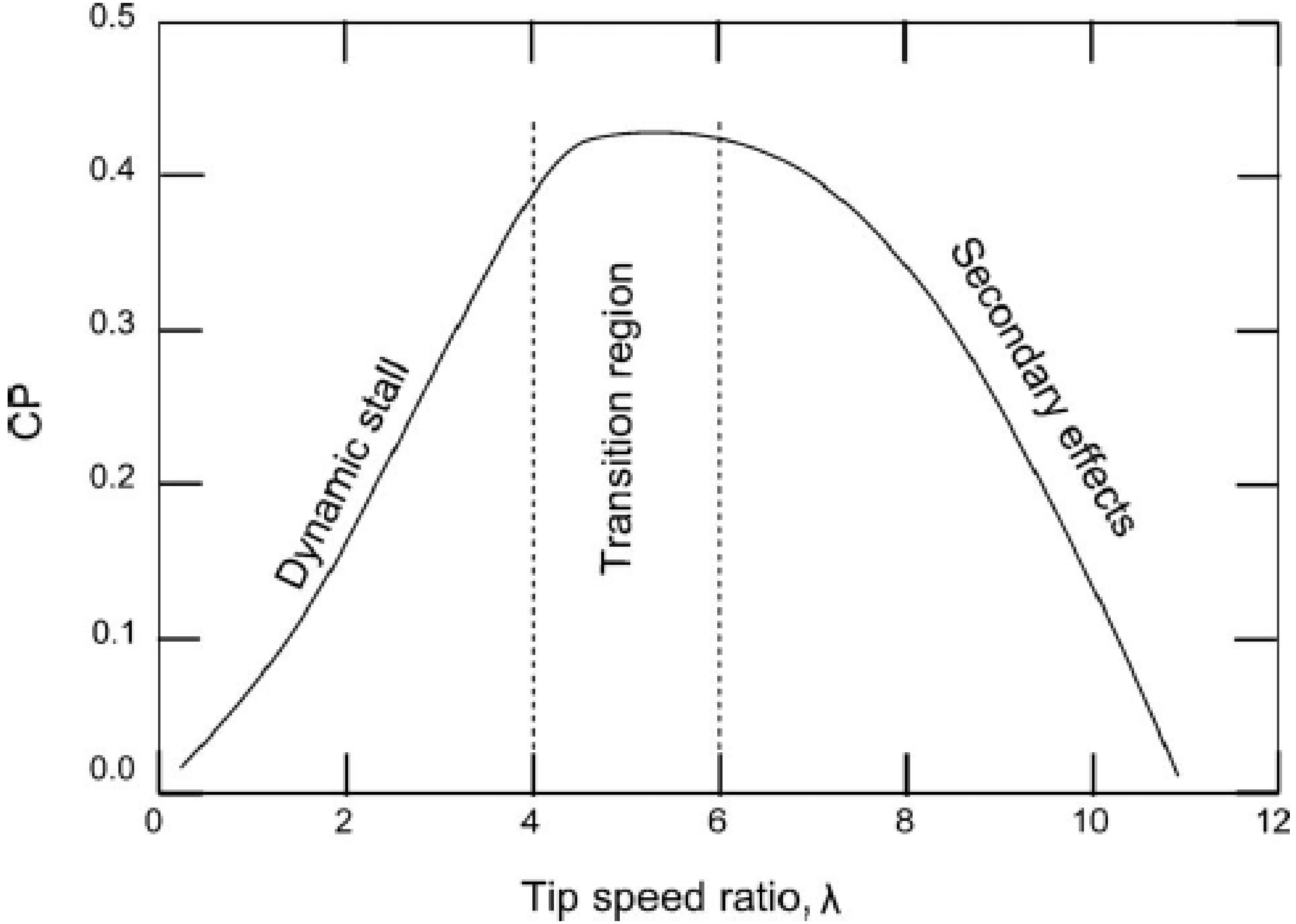

Effect of Turbine Radius on The Power Coefficient

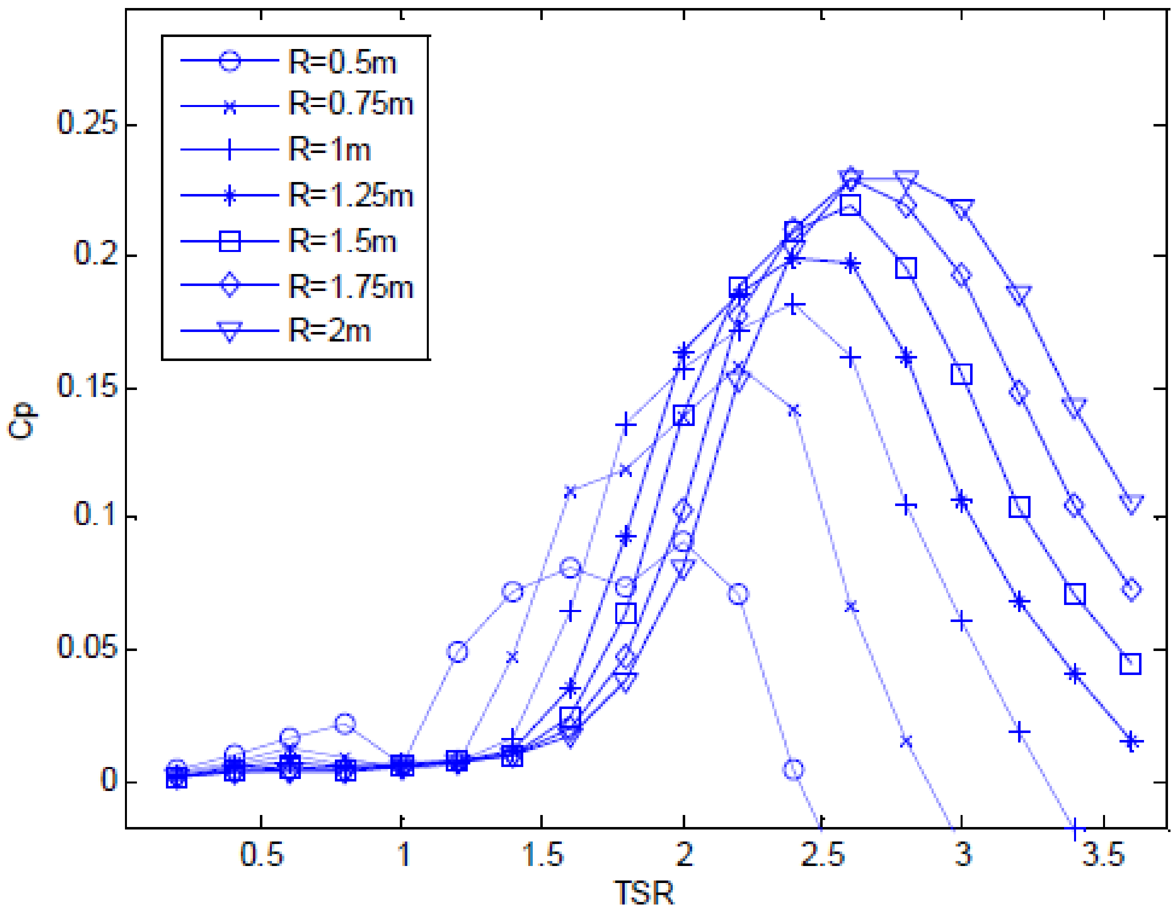

At low tip speed ratios there is no effect for the turbine radius on the Power Coefficient

Induced Speed Vs Azimuth Angle

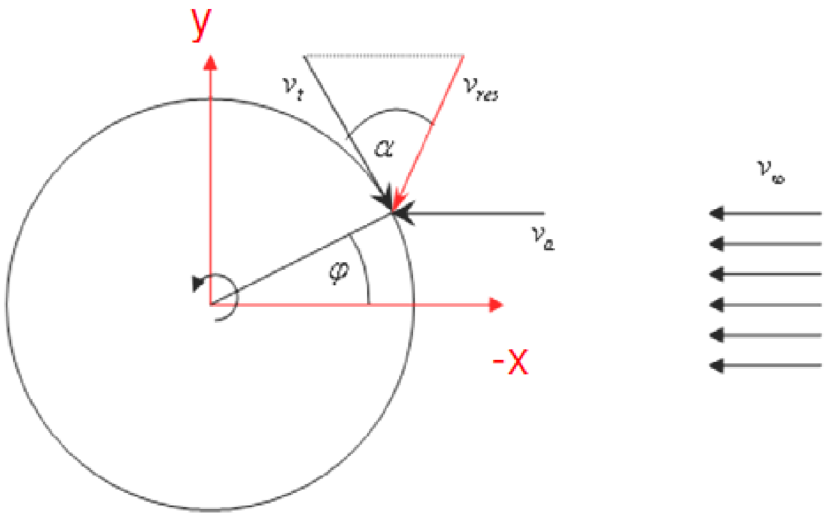

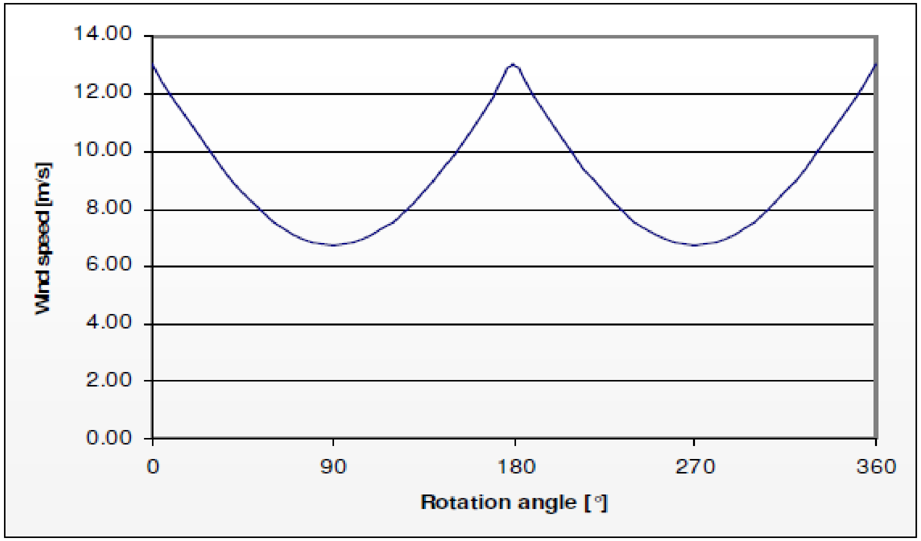

The induced wind speed v_a is given by

$$v_a = v_\infty (1 - a)$$

with the reduction factor

$$a = X \cdot \frac{r \cdot \omega_{rated}}{v_\infty} \left|\sin(\varphi)\right|$$

and the Wilson-Factor

$$X = \frac{B \cdot c}{2r}$$

The lift (F_L) and the drag (F_D) force are given by:

$$F_L = C_L \cdot \frac{\rho}{2} \cdot v_{res}^{\ 2} \cdot A_{bl}$$

$$F_D = C_D \cdot \frac{\rho}{2} \cdot v_{res}^{\ 2} \cdot A_{bl}$$

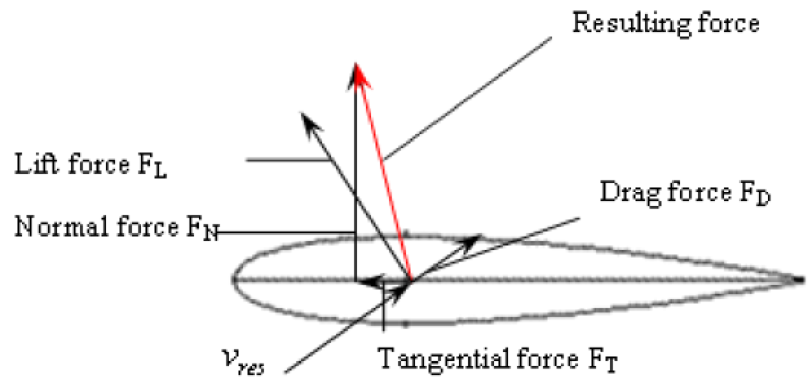

$$F_N = F_L \cdot \cos(\alpha) + F_D \cdot \sin(\alpha)$$

$$F_T = F_L \cdot \sin(\alpha) - F_D \cdot \cos(\alpha)$$

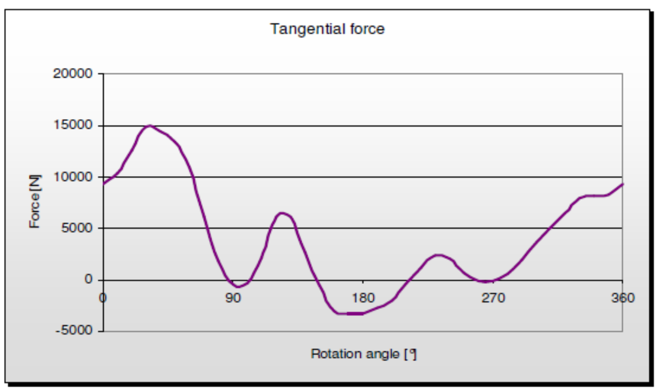

Fig 4: Tangential force vs. rotation angle

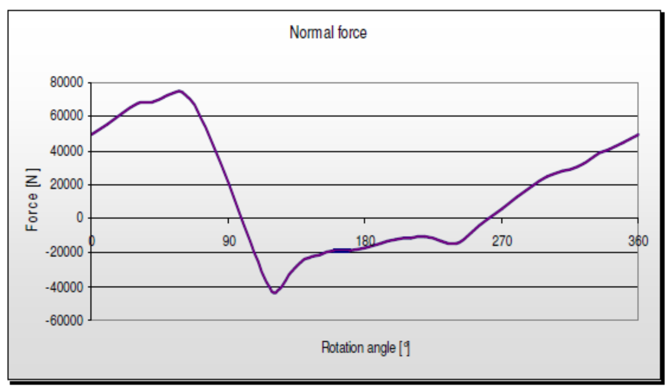

Fig 5: Normal force vs. rotation angle

Why the Savonius turbine cannot be modeled with simple momentum theory

The performance of a single Savonius turbine utilizes the interactive flow between the two blades:

1) The flow attachment to the convex surface of the advancing blade produces a low-pressure region above it to pull the blade in torque-adding direction, i.e. the lift effect at a low tip-speed ratio

3) A large vortex is slowly shed behind the returning blade, which produces low-pressure downstream of the advancing blade.

Second Row

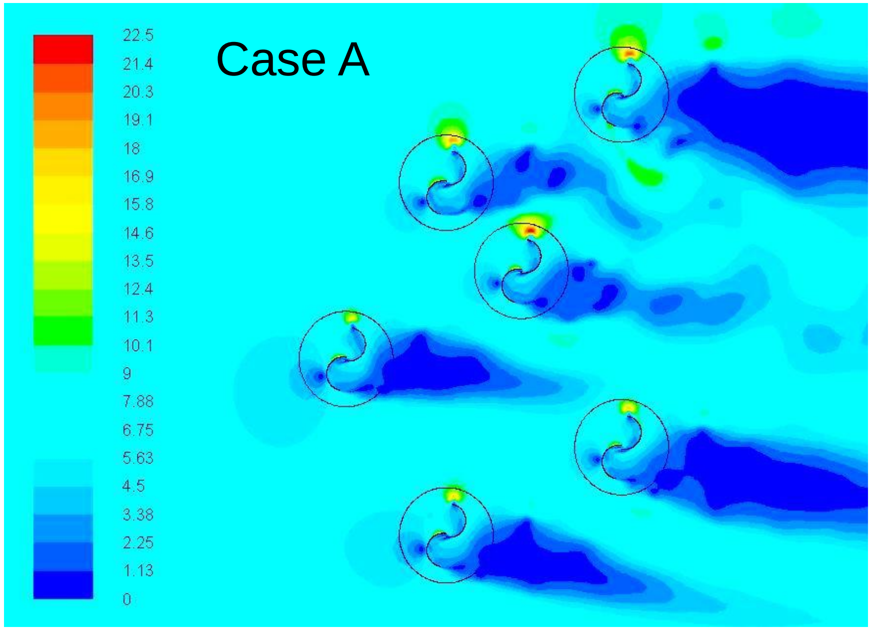
Case A
22.5
21.4
20.3
19.1
18
16.9
15.8
14.6
13.5
12.4
11.3
10.1
9
7.88
6.75
5.63
4.5
3.38
2.25
1.13
0

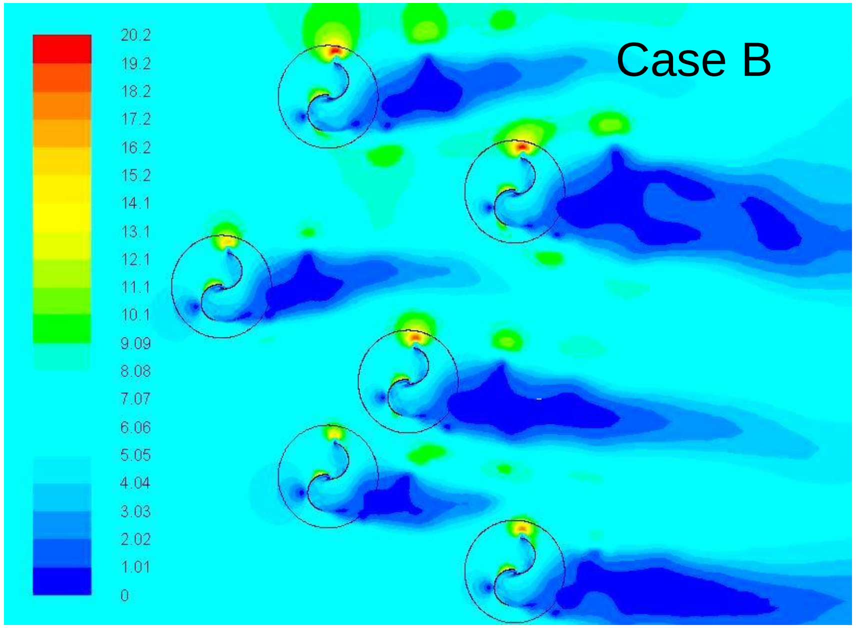
Case B
20.2
19.2
18.2
17.2
16.2
15.2
14.1
13.1
12.1
11.1
10.1
9.09
8.08
7.07
6.06
5.05
4.04
3.03
2.02
1.01
0

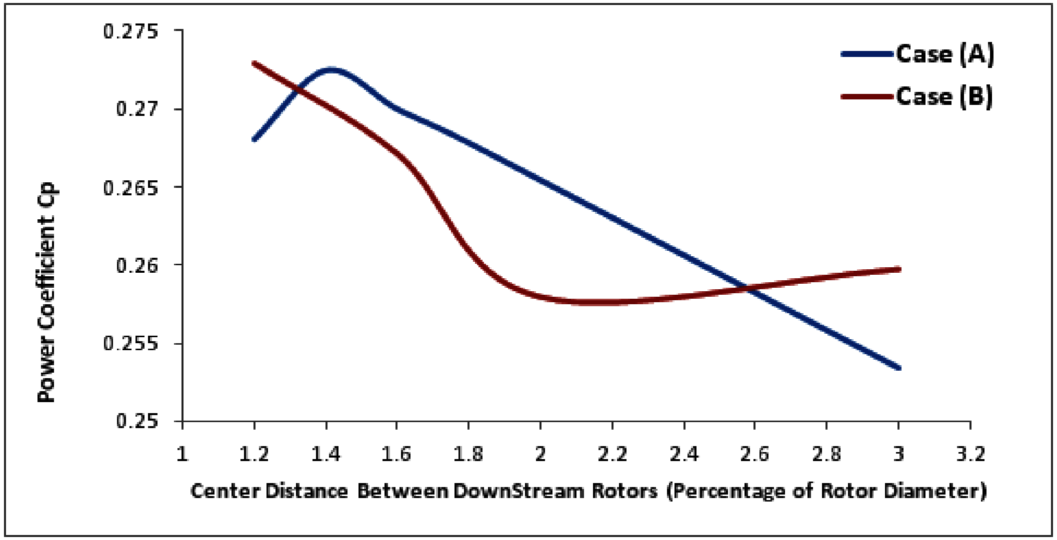
Case (A)
Case (B)
Power Coefficient Cp
0.275
0.27
0.265
0.26
0.255
0.25
1
1.2
1.4
1.6
1.8
2
2.2
2.4
2.6
2.8
3
3.2
Center Distance Between DownStream Rotors (Percentage of Rotor Diameter)

Vorticity equation

$$\frac{D\vec{\omega}}{Dt} = \frac{\partial\vec{\omega}}{\partial t} + (\vec{u}\cdot\nabla)\vec{\omega}$$

The circulation around a closed contour is given by

$$\Gamma = \int_C \vec{U} \cdot \vec{dl} \ .$$

The lift per unit span is related to the circulation by the Kutta-Joukowski theorem of lift,

$$L = \rho \, U_\infty \, \Gamma \ ,$$

2.2 Prandtl's Lifting Line Theory

According to the Prandtl lifting line theory [Von Mises, 1959], a finite wing may be represented by a single equivalent line of vorticity known as the "bound vortex," since it is in a sense bound to the wing. The strength of this vortex, $\Gamma(y)$, is related to the lift distribution along the wing by the Kutta-Joukowski relationship:

$$L(y) = \rho \, U \, \Gamma(y) \ . \qquad (2.3)$$

Two-dimensional flow equation

$$\frac{\partial u}{\partial t} + u\frac{\partial u}{\partial x} + v\frac{\partial u}{\partial y} = -\frac{1}{\rho}\frac{\partial p}{\partial x} + \nu\left(\frac{\partial^2 u}{\partial x^2} + \frac{\partial^2 u}{\partial y^2}\right),$$

$$\frac{\partial v}{\partial t} + u\frac{\partial v}{\partial x} + v\frac{\partial v}{\partial y} = -\frac{1}{\rho}\frac{\partial p}{\partial y} + \nu\left(\frac{\partial^2 v}{\partial x^2} + \frac{\partial^2 v}{\partial y^2}\right),$$

$$\frac{\partial u}{\partial x} + \frac{\partial v}{\partial y} = 0,$$

Axial Induction Factor

The fraction by which the axial component of velocity is reduced is known as the axial induction factor (a*).*

If the free stream velocity is U_∞ and the axial velocity at the rotor plane is U_1 , then the axial induction factor is,

$$a = \frac{U_\infty - U_1}{U_\infty}.$$

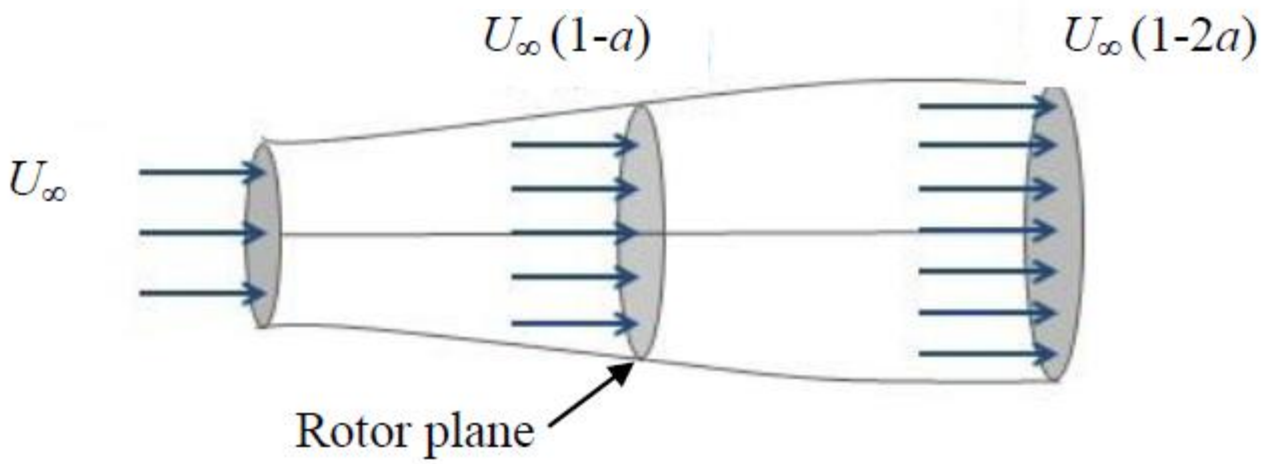

The power W extracted by the wind turbine is related to the axial induction factor (a):

$$\dot{W} = \frac{1}{2}\rho A U_\infty^3 4a(1-a)$$

Tangential induction factor

The tangential induction factor (*a'*) *which is due to rotation of the flow in the wake.*

$$a' = \frac{\omega}{2\Omega},$$

where Ω *is the angular speed of the rotor and* ω *is the angular velocity at which the wake rotates.*

Wall Functions vs. Near-Wall Model

$$y^+ \ (\equiv \rho u_\tau y/\mu)$$

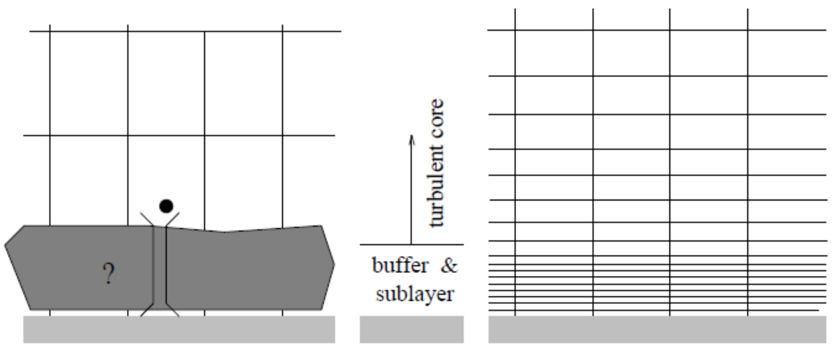

Wall Function Approach

- The viscosity-affected region is not resolved, instead is bridged by the wall functions.
- High-Re turbulence models can be used.

Near-Wall Model Approach

- The near-wall region is resolved all the way down to the wall.
- The turbulence models ought to be valid throughout the near-wall region.

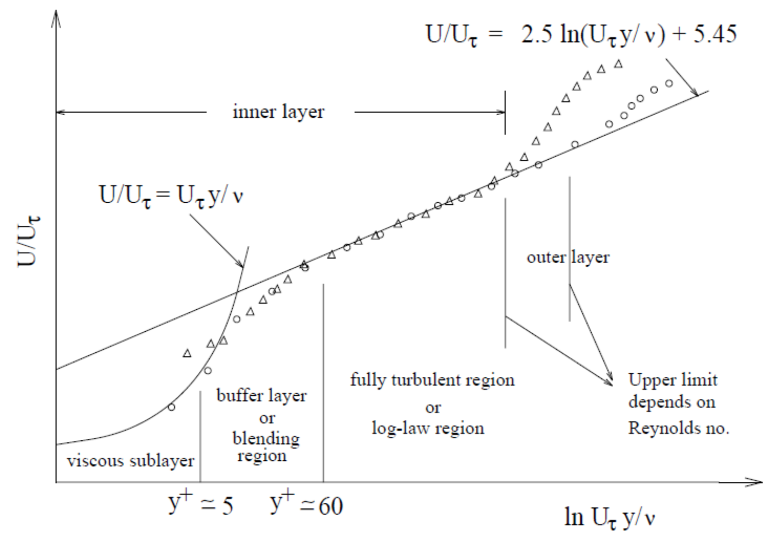

Numerous experiments have shown that the near-wall region can be largely subdivided into three layers. In the innermost layer, called the "viscous sub-layer", the flow is almost laminar, and the (molecular) viscosity plays a dominant role in momentum

"wall functions" are used to bridge the viscosity-affected region between the wall and the fully-turbulent region.

It is known that the log-law is valid for $y^+ > 30$ to 60.

Dimensionless wall distance (y plus)

$$y^+ \equiv \frac{u_*\, y}{\nu}$$

u_* friction velocity at the nearest wall

y the distance to the nearest wall

ν the local kinematic viscosity of the fluid

$$\mathrm{Re_x} = \frac{\rho U_\infty L}{\mu}$$

$$C_\mathrm{f} = \frac{0.026}{\mathrm{Re}_x^{\ 1/7}}$$

$$\tau_\mathrm{wall} = \frac{C_f\, \rho U_\infty^{\ 2}}{2}$$

$$U_\mathrm{fric} = \sqrt{\frac{\tau_\mathrm{wall}}{\rho}}$$

wall spacing $$\Delta s = \frac{y^+ \mu}{U_\mathrm{fric}\, \rho}$$

http://www.pointwise.com/yplus/

Intermittency Contours

For point surfaces, the value is interpolated from all the mesh nodes of the cell containing the point

$$t = \frac{500\,\mu}{\rho U^2}$$

ANSYS Model based on Intermittency

- Intermittency: $\gamma = \frac{t_{turb}}{t_{lam} + t_{turb}}$
- Laminar flow: $\gamma = 0$
- Turbulent flow $\gamma = 1$
- Transition $0 < \gamma < 1$

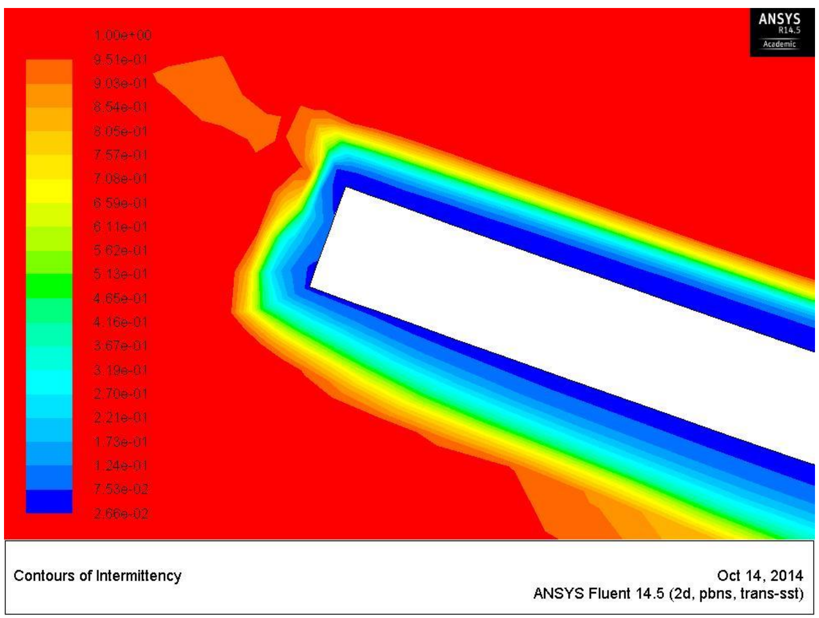

static

Average Intermittency on the blades 0.9

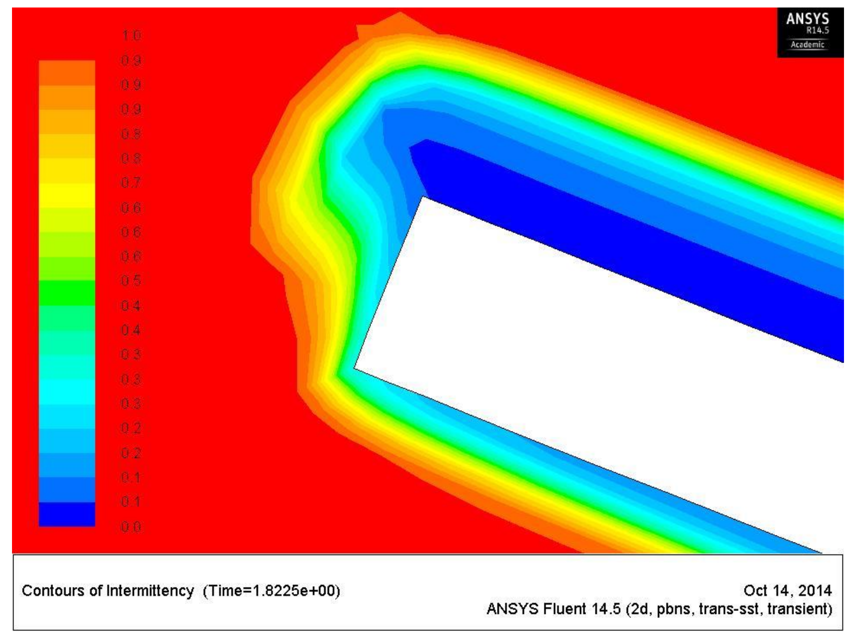

Rotating

Average Intermittency on the blades 0.4

Contours of Turbulence Intensity

K-w (SST model) full turbulent

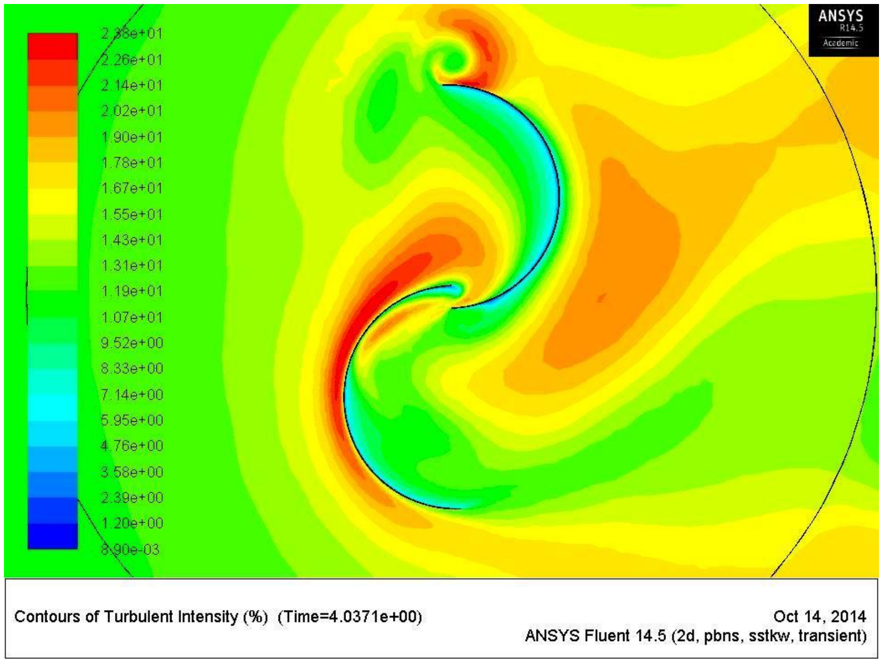

K-w (Trans SST model)

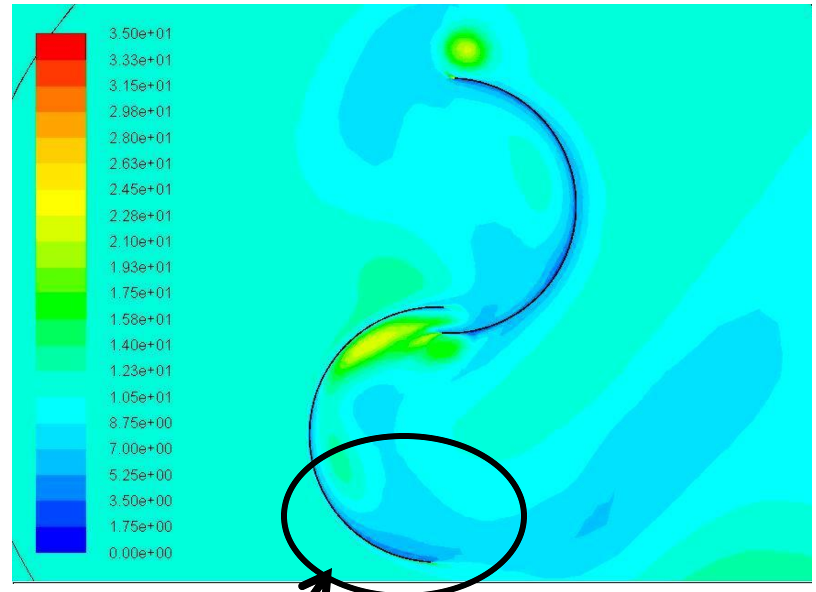

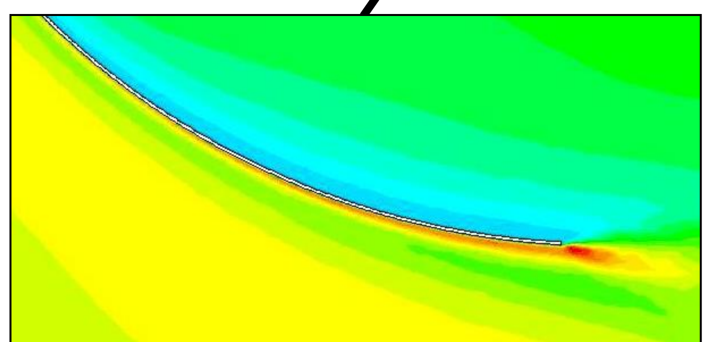

Magnification of Transition Position

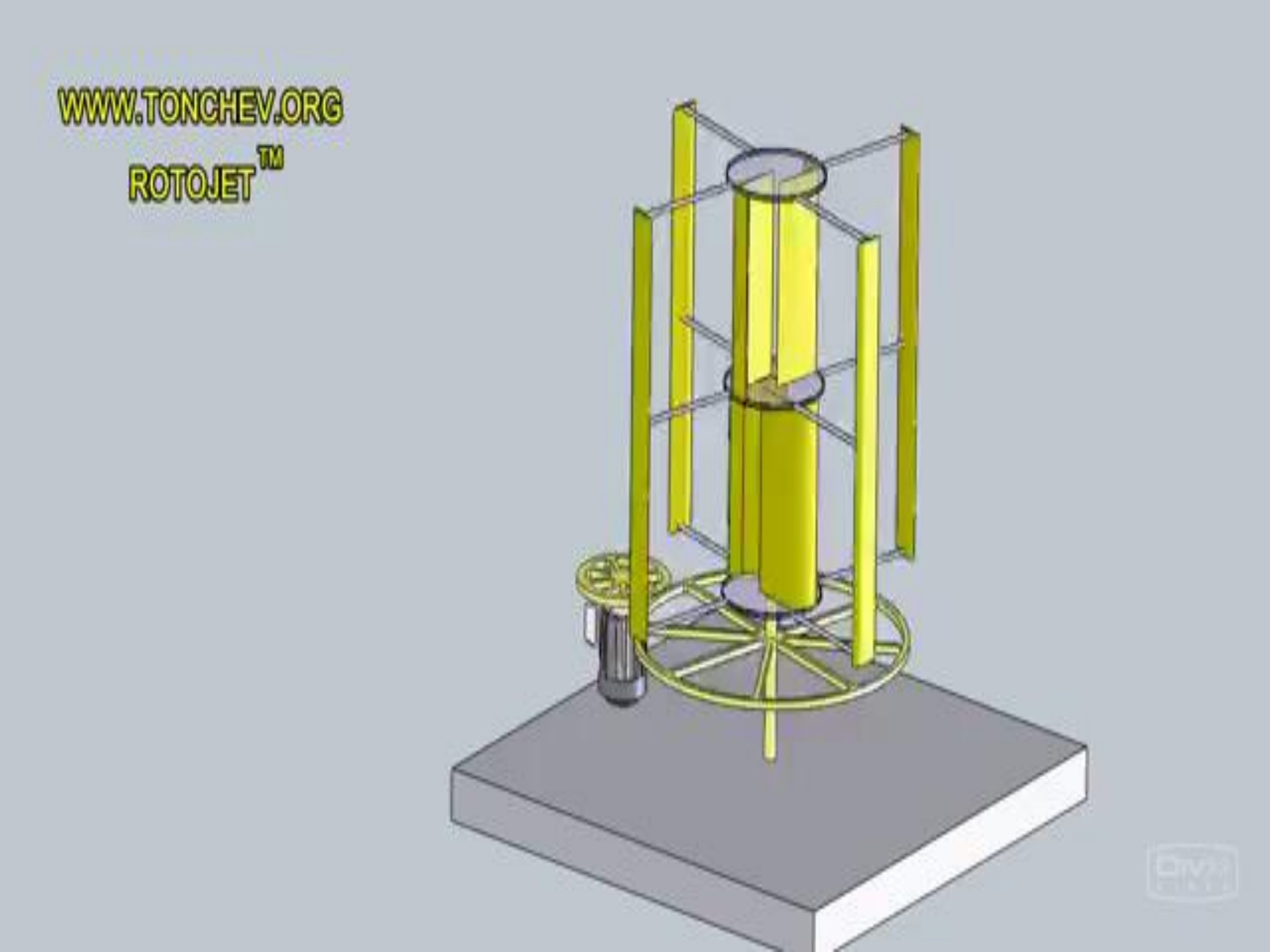
WWW.TONCHEV.ORG
ROTOJET™


Power is generated from the wind or from the current, or from both.
Adaptable to meet varying metocean conditions.
3
2
A gearbox transmits the increased rotation to the Darrieus Wind Turbine.
No External power is required for startup.
1
The Savonius Current Turbine harnesses the energy produced by the ocean currents.

Experimental Data Correction

An object placed in a wind tunnel produces some "tunnel blockage"

This causes the local wind velocity in the test section to increase.

This increase has to be accounted for by determining a tunnel blockage factor (ε)

The total tunnel blockage correction be determined by applying the following equation:

$$\epsilon = \frac{1}{4} \frac{\text{Model frontal area}}{\text{Test section area}}$$

Pope, A. and Harper, J.J., *Low Speed Wind Tunnel Testing,* John Wiley, New York, 1966.

$$V_\infty = V_{\infty_u} (1 + \epsilon)$$

$$q_\infty = q_{\infty_u} (1 + \epsilon)^2$$

Tip speed ratio

$$X_\infty = R\Omega / V_\infty$$

Torque coefficient

$$C_Q = (Q + Q_f) / \tfrac{1}{2}\rho_\infty V_\infty^2 R A_s$$

Power coefficient

$$C_P = (Q + Q_f)\Omega / \tfrac{1}{2}\rho_\infty V_\infty^3 A_s$$

My Status

- Arrived at USA on 23 September 2012
- Did written qualifier exam on November 2013
- Finished courses on December 2013, with GPA: 3.833
- Did oral qualifying exam on January 2014
- Did proposal defense on October 2014